GLIA 54:606–618 (2006)

Extracellular ATP Counteracts the ERK1/2-Mediated Death-Promoting Signaling Cascades in Astrocytes

YOUICHI SHINOZAKI,[1] SCHUICHI KOIZUMI,[1] YASUO OHNO,[2] TAKU NAGAO,[2] AND KAZUHIDE INOUE[3]*
[1]*Division of Pharmacology, National Institute of Health Sciences, Setagaya, Tokyo 158-8501, Japan*
[2]*National Institute of Health Sciences, Setagaya, Tokyo 158-8501, Japan*
[3]*Department of Molecular and System Pharmacology, Graduate School of Pharmaceutical Sciences, Kyushu University, Higashi-ku, Fukuoka 812-8582, Japan*

KEY WORDS
purinergic receptor; oxidative stress; ERK1/2; src family; protein tyrosine phosphatase

ABSTRACT
Oxidative stress is the main cause of neuronal death in pathological conditions. Hydrogen peroxide (H_2O_2), one of the reactive oxygen species, activates many intracellular signaling cascades including src family and mitogen-activated protein kinases (MAPKs), some of which are critically involved in the induction of cellular damage. We previously showed that H_2O_2-induced cell death in astrocytes and adenosine 5′-triphosphate (ATP), acting on $P2Y_1$ receptors, had a protective effect. Here, we examined the H_2O_2-induced changes in intracellular signaling cascades that promote cell death in astrocytes, showing the molecular mechanisms by which the activation of $P2Y_1$ receptors counteracts such signals. Although H_2O_2 activated three MAPKs including ERK1/2, p38, and JNK, only the activation of ERK1/2 participated in the H_2O_2-evoked cell death. H_2O_2 induced a sustained activation of ERK1/2 mainly in the nucleus region, which was well in accordance with the H_2O_2-induced cell death. H_2O_2 also activated the src tyrosine kinase family, which was an upstream signal for ERK1/2. Activation of $P2Y_1$ receptors by 2methylthio-ADP (2MeSADP) inhibited the H_2O_2-evoked activation of src tyrosine kinase, resulting in the inhibition of the phosphorylated-ERK1/2 accumulation in the nucleus. 2MeSADP enhanced the gene expression and activity of protein tyrosine phosphatase (PTP), which was responsible for the inhibition of src tyrosine kinase. Thioredoxin reductase, another cytoprotective gene we previously showed to be upregulated by 2MeSADP, also controlled the activity of PTP. Taken together, ATP, acting on $P2Y_1$ receptors, upregulates the PTP expression and its activity, which counteracts the H_2O_2-promoted death signaling cascades including ERK1/2 and its upstream signal src tyrosine kinase in astrocytes.

INTRODUCTION

Adenosine 5′-triphosphate (ATP) is an important signaling molecule that mediates gliotransmission and also glia-to-neuron communication in the CNS (Fields and Stevens-Graham, 2002; Hansson and Ronnback, 2003; Inoue, 2002). The $P2Y_1$ receptor has a central role in the ATP-mediated gliotransmission in astrocytes (Fam et al., 2000) and we previously demonstrated that ATP, acting on $P2Y_1$ receptors, protected astrocytes against oxidative stress, indicating the physiological importance of ATP-mediated gliotransmission in astrocytes (Shinozaki et al., 2005). However, details concerning the molecular mechanism(s) by which $P2Y_1$ receptor activation results in such protection are still lacking.

Hydrogen peroxide (H_2O_2), one of the reactive oxygen species (ROS), activates various intracellular signaling cascades including mitogen-activated protein kinases (MAPKs) (Fialkow et al., 1994; Konishi et al., 1999; Ushio-Fukai et al., 1999). The MAPK family includes extracellular signal-regulated kinase 1 and 2 (ERK1/2), p38 kinase, and c-Jun NH_2-terminal kinase (JNK). The latter two members are well known to be stress-responding MAPKs, which are activated by lipopolysaccharide, cytokines, and oxidative stress such as by H_2O_2 and induce cell death (Oppenheim, 1991). ERK1/2 is constitutively expressed in various regions including the CNS (Boulton et al., 1991). ERK1/2 is activated by various neurotransmitters, hormones and growth factors in physiological conditions, controls the transcription factor activity and induces various physiological responses, such as cell proliferation or differentiation (Boulton et al., 1991; Marshall, 1995; Segal and Greenberg, 1996). However, ERK1/2 is also activated by various types of stress such as oxidative stress or shear stress, and appears to control the survival of cells (Guyton et al., 1996; Takahashi and Berk, 1996; Wang et al., 1998; Xia et al., 1995). Concerning neuronal cells, recent reports have shown that activation of ERK1/2 even promotes cell death both in vivo and in vitro (Murray et al., 1998; Namura et al., 2001; Stanciu and DeFranco, 2002; Subramaniam et al., 2004). Thus, although ERK1/2 is an essential intracellular signaling molecule that mediates various physiological functions, it may also mediate the death of cells. The intensity of ERK1/2 activation and spatial and temporal differences in its activation would greatly affect physiological or pathophysiological events in cells.

The src family, a well-known protein tyrosine kinase (PTK), regulates a variety of cellular functions such as cell

Grant sponsor: The National Institute of Biomedical Innovation, MF-16 grant; Grant sponsor: Uehara Memorial Foundation; Grant sponsor: Scientific Research (B) for Young Scientists (A) and on Priority Areas (A), Ministry of Education, Science, Sports and Culture, Japan.

*Correspondence to: Kazuhide Inoue, Department of Molecular and System Pharmacology, Graduate School of Pharmaceutical Sciences, Kyushu University, Maidashi 3-1-1, Higashi-ku, Fukuoka 812-8582, Japan.
E-mail: inoue@phar.kyushu-u.ac.jp

Received 1 December 2005; Revised 21 July 2006; Accepted 25 July 2006

DOI 10.1002/glia.20408

Published online 30 August 2006 in Wiley InterScience (www.interscience.wiley.com).

growth, proliferation, and differentiation. The src family is abundantly expressed in the CNS (Brugge et al., 1985; Sugrue et al., 1990), and is also involved in brain injury induced by oxidative stress. In fact, H_2O_2 or ischemia/reperfusion injury activates the src family in the hippocampus (Guo et al., 2003; Ohtsuki et al., 1996). Activation of the src family is prevented by protein tyrosine phosphatase (PTP). PTP is related to various events in the CNS such as inhibition of the NMDA receptor activation in neurons(Yu and Salter, 1999) and of microglial TNFa and nitric oxide generation by amyloid β (Tan et al., 2000). In addition, PTP upregulation is observed in kainic acid-treated (Boschert et al., 1997) and ischemia-injured neurons (Takano et al., 1996). Thus, the activity and expression of PTP is also important for the regulation of pathophysiological cellular functions as well as the regulation of src tyrosine kinase.

On the basis of these findings, we hypothesized that MAPKs and src family are key molecules for promoting the H_2O_2-evoked cell death in astrocytes and that ATP acting on $P2Y_1$ receptors may counteract these cell death-promoting signaling cascades.

In the present study, we demonstrate that activation of both src tyrosine kinase and the subsequent ERK1/2 are key events in the H_2O_2-evoked cell death in astrocytes. We also demonstrate that ATP/$P2Y_1$ receptor activation interferes with the H_2O_2-evoked src family—ERK1/2 cascades by increasing the expression and activity of PTP, thereby leading to protection against H_2O_2-induced cell death in astrocytes.

MATERIALS AND METHODS

Chemicals

Adenosine 5′-triphosphate (ATP), adenosine, 2-methylthio adenosine diphosphate (2MeSADP), bovine serum albumin (BSA), propidium iodide (PI), sodium orthovanadate (Na_3VO_4), MRS2179, and *N*-acetyl cystein were purchased from Sigma Chemical (St Louis, MO). The sources of other chemicals are shown in parentheses as follows; hydrogen peroxide (H_2O_2) (Wako Pure Chemicals, Osaka, Japan), 3-(4,5-dimethylthiazol-2-y1)-2,5-diphenyltetrazolium bromide (MTT) assay kit (CHEMICON International, Temecula, CA), PD98059, U0126, SB203580, SP600125, and PP3 (Calbiochem Biosciences, San Diego), PP1 and PP2 (Biosource, CA), auranofin (Alexis biochemicals, Lausen, Switzerland).

Abbreviations

ATP	adenosine 5′-triphosphate
2MeSADP	2-methylthio-adenosine 5′-diphosphate
ERK1/2	extracellular signal-regulated kinase 1 and 2
H_2O_2	hydrogen peroxide
JNK	c-Jun NH_2-terminal kinase
MAPK	mitogen-activated protein kinase
MAPKP	MAPK phosphatase
MEK1/2	MAPK kinase 1 and 2
Na_3VO_4	sodium orthovanadate
PI	propidium iodide
PTK	protein tyrosine kinase
PTP	protein tyrosine phosphatase
P-Tyr	phosphorylated tyrosine
ROS	reactive oxygen species
TrxR	thioredoxin reductase

Antibodies

Polyclonal antibodies against total ERK1/2, phosphorylated ERK1/2, phosphorylated p38, and phosphorylated JNK were purchased from Cell Signaling Technology (Beverly, MA). The monoclonal antibody against phosphorylated tyrosine was purchased from Sigma Chemical (St Louis, MO).

Cells and Cell Culture

Astrocytes were prepared from neonatal rat forebrain. The cells were cultured as previously reported (Shinozaki et al., 2005). For the cell viability assay, cells were seeded on 96-well plates (NUNC, Roskilde, Denmark) at a density of 1.25×10^4 cells/well.

Cell Viability Assay

For the cell viability assay, we used an MTT assay as previously reported (Shinozaki et al., 2005). A 1/10 volume of MTT solution (5 mg/mL in PBS) was added and incubated for 4 h under 10% CO_2/90% air at 37°C. Then, an equal volume of isopropanol (with 0.04 N HCl) was added to the cells. The absorbance was measured on an ELISA plate reader (ASYS Hitech, Eugendorf, Austria) with a test and reference wavelength of 570 and 630 nm, respectively.

Western Blotting

Astrocytes were prepared as described above. After H_2O_2-stimulation, cells were lysed and the lysates were resolved with 10% SDS-PAGE gels and transferred to PVDF membranes. The membranes were blocked for 1 h in Tris-buffered saline containing 0.1% Tween-20 (TBS/T) and 5% non-fat dry milk at room temperature. Then the membranes were incubated with primary antibody dilution buffer (1:1000 dilution into TBS/T containing 5% BSA) overnight at 4°C. After three washes with TBS/T, the membranes were incubated with horseradish peroxidase-conjugated anti-rabbit antibody (1:2000 dilution into TBS/T containing 5% non-fat dry milk) for 1 h at room temperature. The membranes were washed with TBS/T three times, and the proteins were visualized by chemiluminescence. The antibodies for anti-phospho-proteins used in the present study (anti-P-ERK1/2, P-p38, and P-JNK or P-Tyr antibodies) specifically detected only the activated and phosphorylated form of the proteins. To detect total ERK1/2, the aliquot of the same sample was resolved with 10% SDS-PAGE gels, transferred to PVDF membranes in the same conditions and exposed to anti-total ERK1/2 antibody.

Quantification of the Intensity of P-ERK1/2 Bands

To quantify the intensity of P-ERK1/2 bands, we used Image J (http://rsb.info.nih.gov/ij/). P-ERK1/2 bands were selected by rectangular selection. Then, we selected *Analyze-Gels-Select First Lane* from the menu bar. The

area corresponding to each band was measured using *Wand (tracing) tool* from the tool bar.

Immunocytochemistry

After each treatment, the cells were fixed for 30 min at room temperature in 3.7% paraformaldehyde. The fixed cells were permeabilized with PBS containing 0.1% Triton X-100 for 5 min at room temperature and then incubated with the polyclonal anti-ERK1/2 and anti-phospho-ERK1/2 antibodies for 24 h at 4°C. After washing, the cells were incubated with the appropriate secondary antibodies conjugated to Alexa 488 or 546, washed again, and mounted on glass coverslips (Matsunami Glass, Osaka, Japan). Astrocytes for immunocytochemistry were selected randomly. Images were collected in an MRC-1024 laser-scanning microscope (Bio-Rad) with 20× objective lenses. For the comparison of double-stained patterns, images were processed using Photoshop 5 (Adobe System, Mountain View, CA).

Tyrosine Phosphatase Assay

The tyrosine phosphatase activity was measured using a universal tyrosine phosphatase kit (Takara, Shiga, Japan). The measurement was done according to the manufacturer's instructions. Cells were lysed by lysis buffer and transferred into 96-well ELISA plates at a volume of 50 μL/well followed by incubation for 45 min at 37°C. After four times washing with tween-PBS (PBS containing 0.05% tween20), blocking buffer was added to the wells at a volume of 100 μL/well followed by 30 min incubation at 37°C. Then, the blocking buffer was discarded and coloring substrates were added to the wells (100 μL/well). After a 15 min incubation at room temperature, 1 N sulfuric acid was added to the wells (100 μL/well) to stop the reaction. The absorbance was measured by a plate reader (ASYS Hitech, Eugendorf, Austria) at a test wavelength of 450 nm.

Quantitative RT-PCR of PTP Genes

RT-PCR amplifications were performed using Taqman One-step RT-PCR Master Mix Reagents and 200 nM PTP specific primers as previously reported (Shinozaki et al., 2005). Using the computer software Primer Express (Applied Biosystems), clone-specific primers were designed to recognized rat PTP genes, i.e., rat PTP4a1 (Taqman probe, 5′-acacaatccaaccaatgcgaccttaaacaa-3′; forward, 5′-tgctcctgtggaagtcacataca-3′; reverse, 5′-gtcgtaagttgcttcgcatactctta-3′) and rat PTPro (Taqman probe, 5′-ccgctatacaaacatcctgccgtacgactt-3′; forward, 5′-ttccgctgaaccgatgtaaaa-3′; reverse, 5′-tgaggtgagttgtagccaggaata-3′). RT-PCR was performed by 30 min reverse transcription at 48°C, 10 min Amplitaq Gold activation at 95°C, then 15-s denaturation at 95°C, 1 min annealing and elongation at 60°C for 40 cycle in a PRISM7700 (Applied Biosystems). Each experiment was performed in triplicate.

RESULTS

MEK1/2 Inhibitors Protect Astrocytes Against H_2O_2-Evoked Cell Death

Figure 1A shows the effect of H_2O_2 on the activation of MAPKs in astrocytes. Western blotting analysis revealed that stimulation of astrocytes with 250 μM H_2O_2 for 2 h resulted in the activation of three MAPKs, i.e., ERK1/2, p38, and JNK (Fig. 1A). We then tested pharmacologically whether the activation of these MAPKs is involved in the H_2O_2-evoked cell death in astrocytes. The H_2O_2-induced decrease in the cell viability of the astrocytes obtained from the MTT assay was always accompanied by the activation of caspase-3, DNA damage, and nucleus condensation (data not shown). Thus, we defined the decrease in cell viability as cell death in astrocytes in the following experiments. MAPK kinase 1/2 (MEK1/2) activates ERK1/2. The MEK1/2 inhibitors PD98059 (10 μM) (Alessi et al., 1995) and U0126 (20 μM) (Favata et al., 1998) strongly inhibited the H_2O_2-evoked cell death (Fig. 1B). The inhibitory

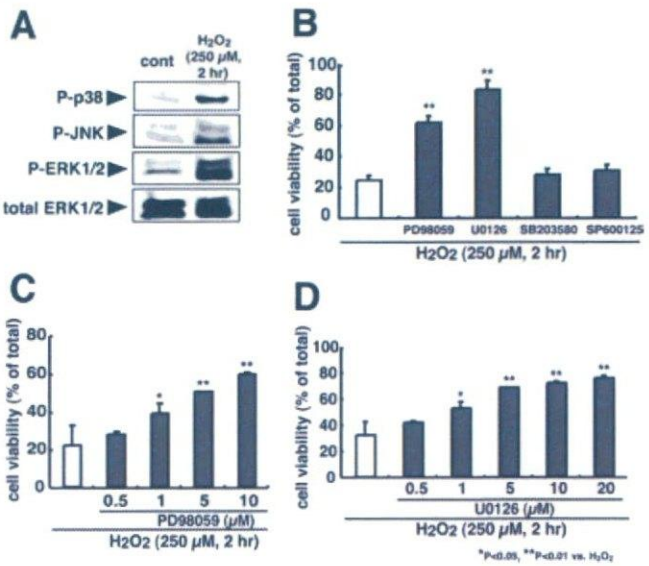

Fig. 1. The effect of MAPK inhibitors on the H_2O_2-evoked cell death of astrocytes. **A**: The effect of H_2O_2 on MAPK activation in astrocytes. H_2O_2 (250 μM, 2 h) activated p38, JNK, and ERK1/2. **B**: The effect of MAPK inhibitors on H_2O_2-evoked cell death. The MEK1/2 inhibitors PD98059 (10 μM) and U0126 (20 μM) strongly inhibited the H_2O_2-evoked cell death. Neither the JNK inhibitor SP600125 (20 μM) nor the p38 inhibitor SB203580 (20 μM) affected the H_2O_2-evoked cell death. **C**: The concentration-dependent effect of PD98059 against H_2O_2-evoked cell death. The protective effect of PD98059 was dose-dependent in a concentration range from 0.5 to 10 μM. **D**: The concentration-dependent effect of U0126 against H_2O_2-evoked cell death. The protective effect of U0126 was dose-dependent in a concentration range from 0.5 to 20 μM. Neither inhibitor alone affected the cell viability of the astrocytes. Inhibitors added to the cells 1 h before H_2O_2 treatment. Asterisks show significant difference from the response evoked by H_2O_2 ($^*P < 0.05$, $^{**}P < 0.01$ vs. H_2O_2 alone, Student's *t*-test). Results were expressed as means ± SEM of triplicate measurements ($n = 3$).

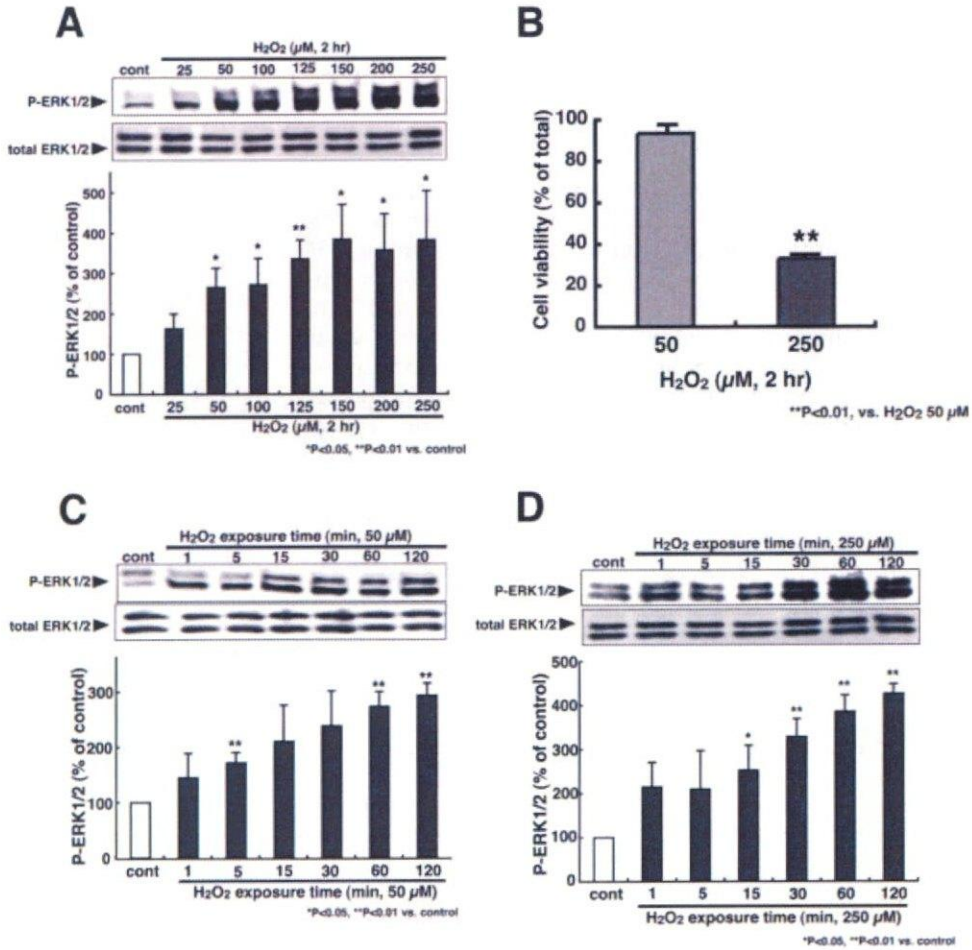

Fig. 2. The concentration-dependency and time course of the H_2O_2-evoked ERK1/2 activation in the astrocytes. **A**: The concentration-dependency of the H_2O_2-evoked ERK1/2 activation. H_2O_2 activated ERK1/2 in a concentration-dependent fashion at the whole cell level (0–250 μM, 2 h). H_2O_2 did not affect the amount of total ERK1/2. Asterisks show significant difference from control (*$P < 0.05$, **$P < 0.01$ vs. control, Student's t-test). **B**: The degree of the decrease of the cell viability of H_2O_2-treated astrocytes markedly decreased the cell viability in the astrocytes 250 μM but not at 50 μM H_2O_2. Asterisks show significant difference from the response evoked by H_2O_2 (**$P < 0.01$ vs. 50 μM H_2O_2, Student's t-test). **C** and **D**: A temporal analysis of the H_2O_2-evoked ERK1/2 activation in the astrocytes. At the whole cell level, ERK1/2 was activated by H_2O_2 treatment time dependently (0–120 min) despite the concentration of H_2O_2 (50 and 250 μM). H_2O_2 did not affect the total ERK1/2. Asterisks show significant difference from control (*$P < 0.05$, **$P < 0.01$ vs. control, Student's t-test). Results were expressed as means ± SEM of triplicate measurements ($n = 3$).

effects by PD98059 and U0126 were dose-dependent in a concentration-range from 0.5 to 10 μM (Fig. 1C) and 0.5 to 20 μM (Fig. 1D), respectively. In contrast, neither the p38 inhibitor SB203580 (Alessandrini et al., 1999; McLaughlin et al., 1996) nor the JNK inhibitor SP600125 (20 μM) (Bennett et al., 2001) had any effect on the H_2O_2-evoked cell death.

The Concentration-Dependency and Time Course of H_2O_2-Evoked ERK1/2 Activation

Among the H_2O_2-activated MAPKs tested, only ERK1/2 was involved in the H_2O_2-evoked cell death (Fig. 1B). H_2O_2 activated ERK1/2 in a concentration- and exposure time-dependent fashion at the whole cell level (Figs. 2A,C,D). Although a lower H_2O_2 concentration (50 μM) activated ERK1/2, H_2O_2 at this concentration did not cause cell death (Fig. 2B). At a higher concentration, H_2O_2 (250 μM) evoked ERK1/2 phosphorylation and cell death in astrocytes (Figs. 2A,B). The phosphorylation of ERK1/2 evoked by 250 μM H_2O_2 was stronger than that evoked by 50 μM H_2O_2. H_2O_2 at either concentration did not affect the total ERK1/2 at the whole cell level.

The Temporal and Spatial Aspect of P-ERK1/2 Induced by H_2O_2

We investigated the temporal and spatial distribution of P-ERK1/2 using immunocytochemical techniques. H_2O_2-evoked ERK1/2 activation was observed in GFAP-positive astrocytes (data not shown). It was reported that ERK1/2 is translocated into the nucleus from the cytoplasm when it is activated (Chen et al., 1992; Gonzalez et al., 1993). We thus analyzed the distribution of P-ERK1/2 after H_2O_2 stimulation. When the cells were stimulated with 250 μM H_2O_2 for 2 h, P-ERK1/2 signals were observed in the center part of individual astrocytes and were colocalized with the signals of PI, a DNA binding dye, suggesting that P-ERK1/2 had translocated into the nucleus (Fig. 3A). In contrast, when stimulated with 50 μM H_2O_2 for 2 h which activated ERK1/2 but did not induce cell death, the P-ERK1/2 signals were observed but were not colocalized with the PI signals (Fig. 3A). The total amount of ERK1/2 signals, however, was not affected by H_2O_2 (50 and 250 μM), and they were not colocalized with the PI signals (Fig. 3B). Without H_2O_2 stimulation, the P-ERK1/2 signals were too low (Figs. 2A,D and 3E, cont.) to detect. To quantify the degree of the colocalization of the P-ERK1/2 and PI signals, we

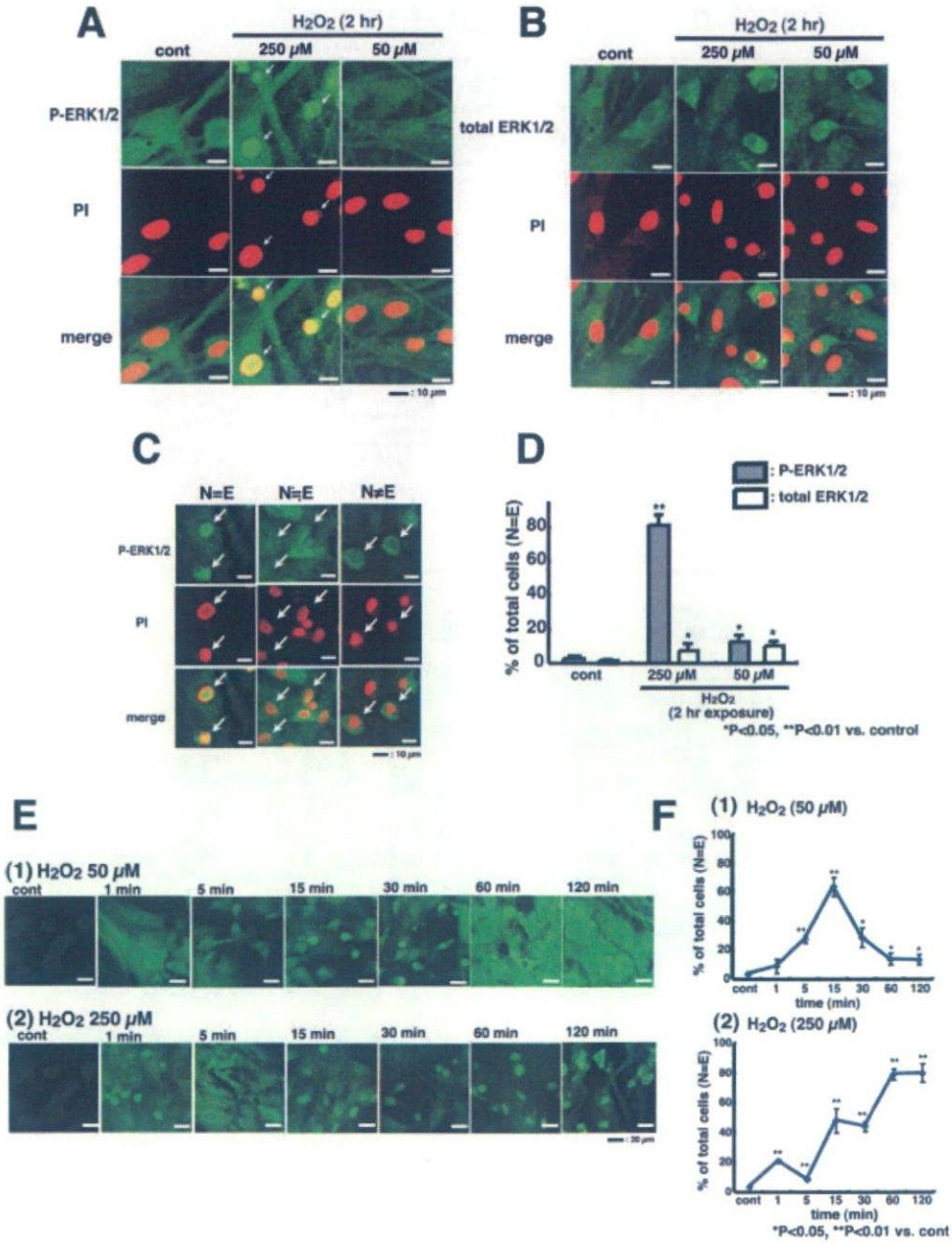

Fig. 3. The effect of H_2O_2 on the intracellular localization of ERK1/2 in astrocytes. **A**: The effect of H_2O_2 on the intracellular localization of P-ERK1/2. In control, the P-ERK1/2 and PI signals did not colocalize (left). When the cells were treated with 250 μM H_2O_2 (2 h), a large number of P-ERK1/2 and PI signals colocalized (center, arrow). At 50 μM H_2O_2, the P-ERK1/2 and PI signals did not colocalize (right). **B**: The effect of H_2O_2 on the intracellular localization of total ERK1/2. Total ERK1/2 did not colocalize with the PI signals irrespective of the H_2O_2 treatment (control, 50 and 250 μM). The signals of P-ERK1/2 were enhanced by photoshop to clarify their intracellular localization. **C**: Classification of the H_2O_2-treated cells into three groups. Astrocytes in which P-ERK1/2 signals were colocalized with PI signals were defined as "N = E" (left), those in which P-ERK1/2 signals were partly colocalized with PI signals were defined as "N =E" (center), and those in which the P-ERK1/2 signals were not colocalized with the PI signals were defined as "N ≠ E" (right). **D**: Quantification of P-ERK1/2 localization into the nucleus. When cells were stimulated by 250 μM H_2O_2, the colocalization of P-ERK1/2 and PI was observed in most cells but not when they were stimulated by 50 μM H_2O_2. Asterisks show significant difference from control ($^*P < 0.05$, $^{**}P < 0.01$ vs. control, Student's *t*-test). **E** and **F**: The temporal analysis of the colocalization of the P-ERK1/2 and PI signals. At 50 μM H_2O_2, N = E cells increased transiently (5–30 min after H_2O_2 stimulation) (E(1), F(1)). At 250 μM H_2O_2, N = E cells increased time-dependently (E(2), F(2)). The DNA binding dye PI was used for identifying the nuclear region. Asterisks show significant difference from control ($^*P < 0.05$, $^{**}P < 0.01$ vs. control, Student's *t*-test). Results were expressed as means ± SEM of triplicate measurements.

classified the cells into three groups, i.e., cells in which P-ERK1/2 signals were colocalized with PI signals (defined as "N = E"), those in which the P-ERK1/2 signals were not colocalized with the PI signals (defined as "N ≠ E"), and P-ERK1/2 signals were partly colocalized with IP signals (defined as "N = E") (Fig. 3C). When stimulated with 50 and 250 μM H_2O_2 for 2 h, the fraction of N = E was 12.7% ± 3.8% (n = 304) and 81.0% ± 6.3% (n = 612), respectively. Without H_2O_2 stimulation, no colocalization of P-ERK1/2 and PI was observed in almost any of the cells (N = E cells, 3% ± 0.2%, n = 346) (Fig. 3D). In contrast to P-ERK1/2, most of the total ERK1/2 signals did not colocalize with PI irrespective of H_2O_2 stimulation(N = E cells, control, 1.3% ± 0.8%, n = 225; 250 μM H_2O_2, 6.5% ± 4.0%, n = 545; 50 μM H_2O_2, 10.7% ± 1.2%, n = 229). Furthermore, we analyzed the time course of the fraction of "N = E" cells after H_2O_2 stimulation. When stimulated with 50 μM H_2O_2, the N = E fraction peaked at 15 min after the stimulation, and the fraction decreased to the prestimulated level after 120 min (N = E cells, 1 min, 7.8% ± 5.4%, n = 201; 5 min, 27.8% ± 2.9%, n = 213; 15 min, 66.6% ± 7.1%, n = 216; 30 min, 29.1% ± 7.4%, n = 226; 60 min, 13.1% ± 4.5%, n = 254; 120 min, 12.7% ± 3.8%, n = 405). In contrast, when stimulated with 250 μM H_2O_2, the N = E fraction gradually increased, reached the maximal level at 60 min, and remained even 120 min after the stimulation (N = E cells, 1 min, 20.7% ± 7%, n = 354; 5 min, 8.1% ± 0.7%, n = 213; 15 min, 48.4% ± 8.3%, n = 220; 30 min, 44.2% ± 3.3%, n = 214; 60 min,

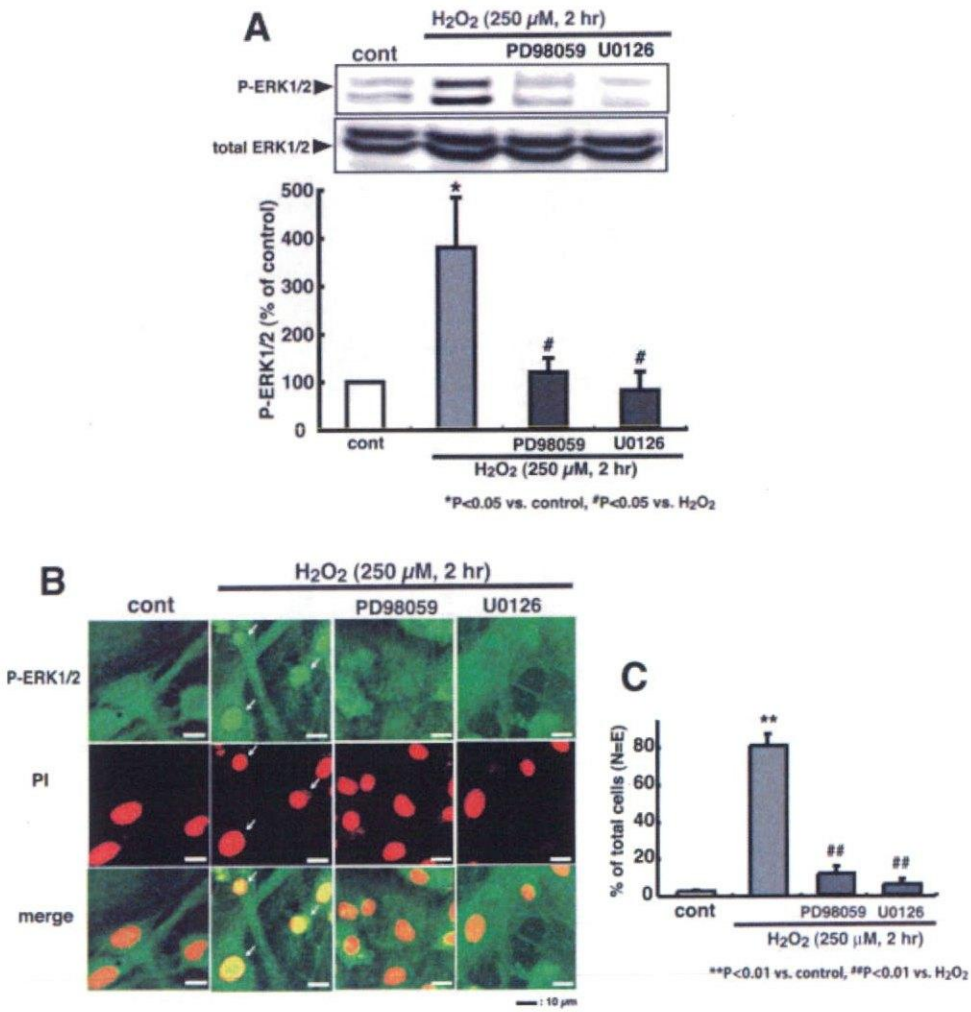

Fig. 4. The effect of MEK1/2 inhibitors on H_2O_2-evoked ERK1/2 activation and P-ERK1/2 translocation. **A**: The effect of MEK1/2 inhibitors on H_2O_2-evoked ERK1/2 activation. PD98059 (10 μM) and U0126 (20 μM) strongly inhibited the H_2O_2-evoked ERK1/2 activation. Asterisks show significant difference from control (*$P < 0.05$ vs. control, Student's *t*-test). Sharps show significant difference from H_2O_2 (#$P < 0.05$ vs. H_2O_2, Student's *t*-test). Results were expressed as means ± SEM of triplicate measurements ($n = 3$). **B** and **C**: The effect of the MEK1/2 inhibitors on the H_2O_2-evoked P-ERK1/2 translocation. PD98059 (10 μM) and U0126 (20 μM) blocked the colocalization of the P-ERK1/2 and PI signals evoked by H_2O_2 (250 μM, 2 h). In the immunocytochemical analysis, the signals of P-ERK1/2 were enhanced by photoshop to clarify their intracellular localization. The DNA binding dye PI was used for identifying the nuclear region. The MEK1/2 inhibitors were applied to the cells 1 h before and during H_2O_2 treatment. Asterisks show significant difference from control (**$P < 0.01$ vs. control, Student's *t*-test). Sharps show significant difference from H_2O_2 (##$P < 0.01$ vs. H_2O_2, Student's *t*-test). Results were expressed as means ± SEM of triplicate measurements.

80.2% ±3.8%, $n = 205$; 120 min, 81%S ± 6.3%, $n = 612$) (Fig. 3F). PD98059 (10 μM) and U0126 (20 μM), at the concentrations that the two inhibitors blocked the H_2O_2-induced cell death (Figs. 1C,D), strongly inhibited the H_2O_2 (250 μM, 2 h)-evoked ERK1/2 activation (Fig. 4A). In addition, these inhibitors prevented the colocalization of P-ERK1/2 and PI, i.e., the H_2O_2-evoked increase in the fraction of N = E was almost abolished (Figs. 4B,C) (N = E cells, PD98059 + H_2O_2, 11.7% ± 3.8%, $n = 524$; U0126 + H_2O_2, 5.9% ± 2.9%, $n = 400$).

ATP Inhibits the H_2O_2-Evoked Activation of ERK1/2 and Its Localization of P-ERK1/2 in the Nucleus

Our previous report by Shinozaki et al., demonstrated that ATP and 2MeSADP inhibited the H_2O_2-induced cell death in astrocytes (Shinozaki et al., 2005). Thus, we examined the effect of ATP and 2MeSADP on the H_2O_2-evoked ERK1/2 activation. In astrocytes pretreated with ATP (100 μM) or 2MeSADP (1 μM) for 24 h, the H_2O_2-induced ERK1/2 activation was markedly inhibited (Fig. 5A). We also analyzed the effect of ATP/2MeSADP on the spatiotemporal behavior of P-ERK1/2 in astrocytes. Immunocytochemical studies showed that pretreatment of the cells with ATP/2MeSADP prevented the H_2O_2-evoked colocalization of P-ERK1/2 and PI signals (Fig. 5B). The fraction of N = E was almost completely inhibited by ATP or 2MeSADP (N = E cells, ATP + H_2O_2, 5.1% ± 3.3%, $n = 340$; 2MeSADP + H_2O_2, 1.1% ± 1.4%, $n = 342$) (Fig. 5C).

ATP itself is known to activate ERK1/2 in some cells including astrocytes (Neary et al., 1999, 2003). Using Western blotting analysis, we found that both ATP (100 μM) and 2MeSADP (1 μM) activated ERK1/2 but the activation was only transient (lasting 1–15 min after stimulation) and returned to the prestimulated level within 120 min [Figs. 6A(i,ii)]. Thus, after the initial phosphorylation of ERK1/2 evoked by ATP/2MeSADP the activation should have returned to the prestimulated level when the astrocytes were stimulated with H_2O_2 24 h after ATP-treatment. Interestingly, when 2MeSADP was pretreated with PD98059 (10 μM) or U0126 (20 μM), the 2MeSADP-induced cytoprotective effects against H_2O_2 disappeared (Fig. 6B). Furthermore, using quantitative RT-PCR, we found that U0126 inhibited the 2MeSADP (1 μM, 2 h)-induced upregula-

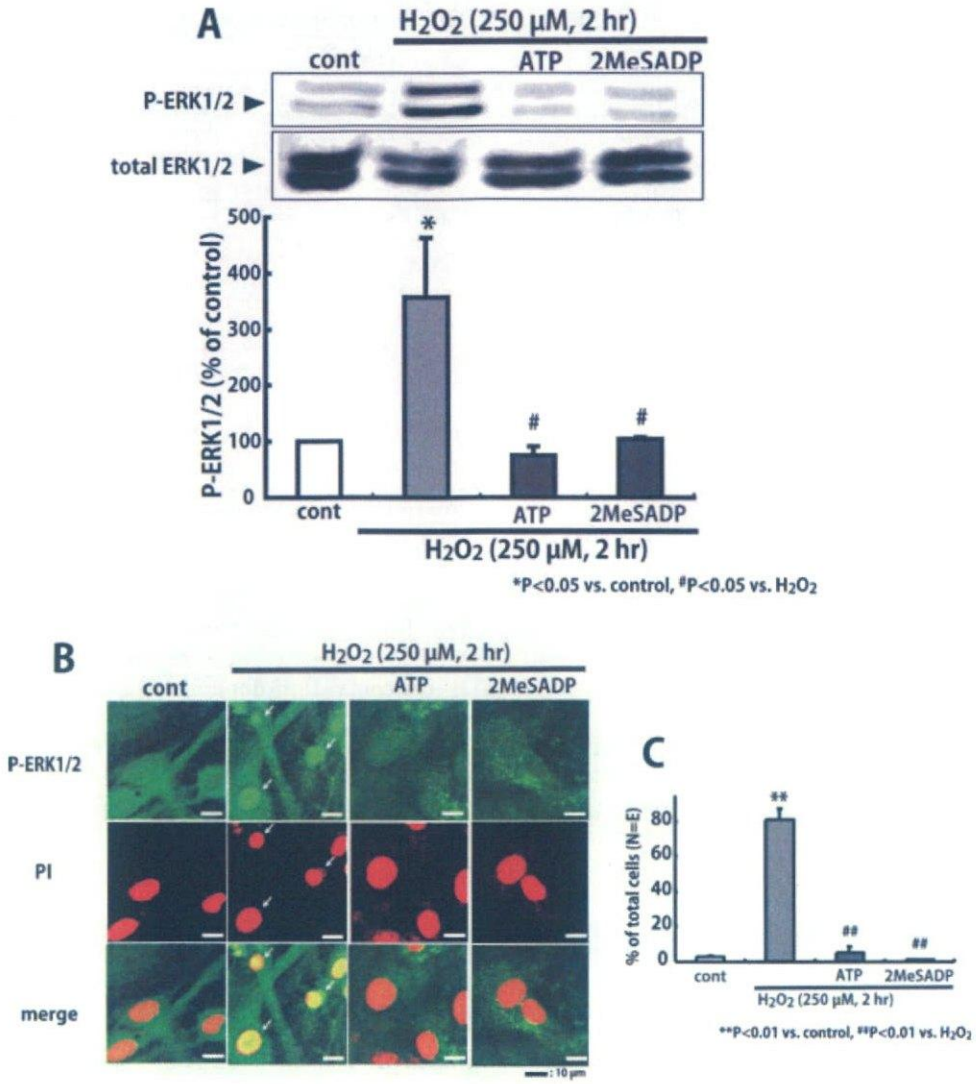

Fig. 5. The effect of ATP and 2MeSADP on H_2O_2-evoked ERK1/2 and P-ERK1/2 translocation. **A**: The effect of ATP and 2MeSADP on H_2O_2-evoked ERK1/2 activation. ATP (100 μM) and 2MeSADP (1 μM) strongly inhibited the H_2O_2-evoked ERK1/2 activation at the whole cell level. Asterisks show significant difference from control ($^*P < 0.05$ vs. control, Student's t-test). Sharps show significant difference from H_2O_2 ($^\#P < 0.05$ vs. H_2O_2, Student's t-test). Results were expressed as means ± SEM of triplicate measurements ($n = 3$). **B** and **C**: The effect of ATP and 2MeSADP on H_2O_2-evoked P-ERK1/2 translocation. ATP (100 μM) and 2MeSADP (1 μM) abolished the colocalization of the P-ERK1/2 and PI signals evoked by H_2O_2 (250 μM, 2 h). In the immunocytochemical analysis, the signals of P-ERK1/2 were enhanced by photoshop to clarify their intracellular localization. The DNA binding dye PI was used for identifying the nuclear region. ATP and 2MeSADP was applied to the cells 24 h before and during H_2O_2 treatment. Asterisks show significant difference from control ($^{**}P < 0.01$ vs. control, Student's t-test). Sharps show significant difference from H_2O_2 ($^{\#\#}P < 0.01$ vs. H_2O_2, Student's t-test). Results were expressed as means ± SEM of triplicate measurements.

tion of thioredoxin reductase (TrxR) (2MeSADP, 232.2% ± 54.4% of control, $P < 0.01$ vs. control; 2MeSADP + U0126, 114.9% ± 9.4% of control, $P < 0.05$ vs. 2MeSADP alone; $n = 3$) and PTPs (PTP4a1: 2MeSADP, 291.1% ± 78.5% of control, $P < 0.05$ vs. control, 2MeSADP + U0126, 102.8% ± 12.2% of control, $P < 0.05$ vs. 2MeSADP alone; $n = 3$; PTPro: 2MeSADP, 608.0% ± 153.8% of control, $P < 0.01$ vs. control; 2MeSADP + U0126, 264.7% ± 47.7% of control, $P < 0.05$ vs. 2MeDADP alone; $n = 3$). U0126 alone did not affect the expression level of TrxR (94.5% ± 30.8% of control; $n = 4$) and PTP genes (PTP4a1, 107.5% ± 21.7% of control; PTPro, 113.6% ± 14.3% of control, $n = 4$). The MEK1/2 inhibitors were added to the cells 1 h before and during 2MeSADP-treatment, and was washed out before the H_2O_2 stimulation. Thus, the phosphorylation of ERK1/2 induced by H_2O_2, represented by the sustained and intense responses seen mainly in the nucleus appeared to cause cell death in the astrocytes, while the ATP-induced transient phosphorylation of ERK1/2 appeared to have a cytoprotective action.

ATP Increases PTP Expression and Its Activity, Leading to Protection Against the H_2O_2-Evoked Cell Death in Astrocytes

We comprehensively studied whether ATP induces the expression of genes that could regulate ERK1/2 activity using a GeneChip microarray. We expected that ATP might upregulate the expression of genes that dephosphorylate ERK1/2 such as MAPK phosphatase (MAPKP), which dephosphorylates ERK1/2, thereby leading to the inactivation of ERK1/2 and the cytoprotective action by ATP. However, no upregulation of any MAPKPs in the GeneChip microarray was observed. Instead, we found the ATP (100 μM, 2 h)-induced upregulation of PTP genes containing PTP4a1 and PTP, receptor type O (PTPro) (Table I).

In the PTP activity assay, both ATP (100 μM, 24 h) and 2MeSADP (1 μM, 24 h) significantly increased the PTP activity (ATP, 148.3% ± 8.8%; 2MeSADP, 168.8% ± 4.8%) (Fig. 7A). Subsequently, we analyzed the effect of the PTP inhibitor sodium orthovanadate (Na_3VO_4)

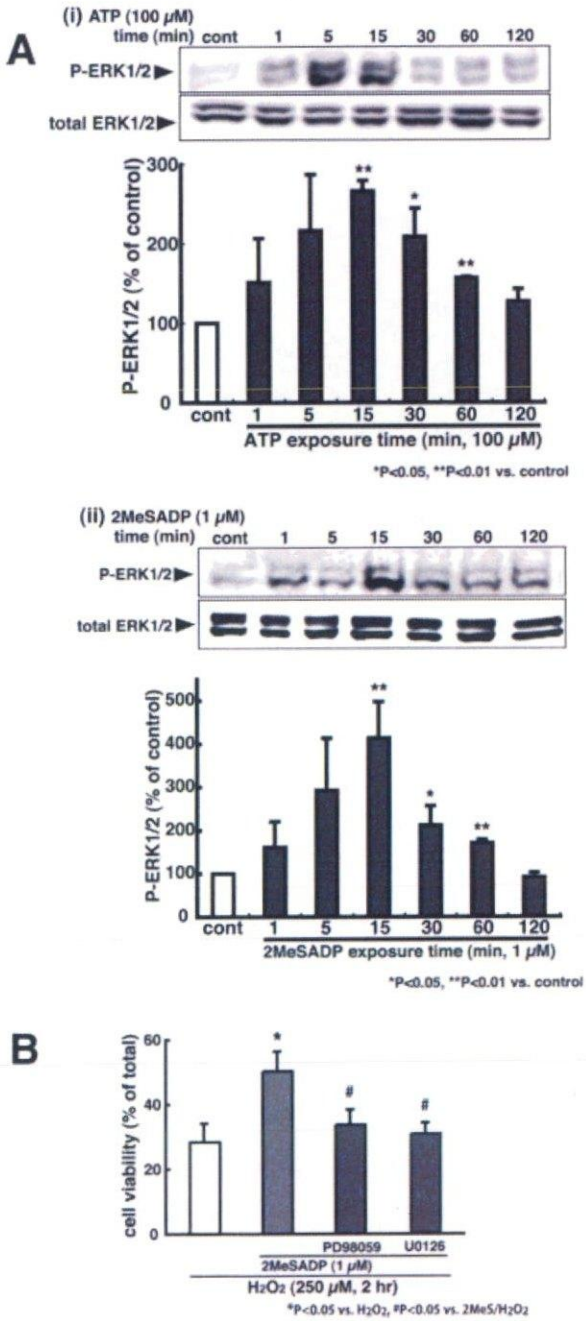

Fig. 6. Analysis of ATP-stimulated ERK1/2 activation in astrocytes. **A**: The time course of ATP-induced ERK1/2 activation. ATP (100 μM) activated ERK1/2 transiently (1–15 min after stimulation) (i). 2MeSADP (1 μM) also activated ERK1/2 transiently (1–15 min after stimulation) (ii). ATP and 2MeSADP did not affect the total amount of ERK1/2. Asterisks show significant difference from control (*$P < 0.05$, **$P < 0.01$ vs. control, Student's t-test). **B**: The effect of 2MeSADP-stimulated ERK1/2 on the $P2Y_1$ receptor-mediated cytoprotective effect. The MEK1/2 inhibitors PD98059 (10 μM) and U0126 (20 μM) strongly inhibited the protective effect induced by 2MeSADP (1 μM, 24 h). The MEK1/2 inhibitors were added to the cells 1 h before the 2MeSADP treatment and were washed out before the H_2O_2 treatment. Asterisks show significant difference from the response evoked by H_2O_2 (*$P < 0.05$ vs. 250 μM H_2O_2, Student's t-test). Sharps show significant difference from 2MeSADP/H_2O_2 (#$P < 0.05$ vs. 2MeSADP/H_2O_2, Student's t-test). Results were expressed as means ± SEM of triplicate measurements ($n = 3$).

TABLE 1. List of PTP Genes Upregulated by ATP in Astrocytes

Title	Fold increase (RT-PCR)	Gene ontology[a]
Protein tyrosine phosphatase 4a1	1.7 (5.7)	Protein tyrosine phosphatase activity (GO:0004725) Nucleus (GO:0005634)
Protein tyrosine phosphatase, receptor type, O	1.8 (4.4)	Protein tyrosine phosphatase activity (GO:0004725) Nervous system development (GO:0007399)
	1.6	Protein tyrosine phosphatase activity (GO:0004725) Nervous system development (GO:0007399)

[a]GO ontology defined by Gene Ontology Consortium (www.godatabase.org/cgi-bin/amigo/go.cgi).

(Heffetz et al., 1990; Shisheva and Shechter, 1993) on the ATP- and 2MeSADP-induced cytoprotective action in astrocytes. Na_3VO_4 concentration-dependently reversed the cytoprotective effect by ATP and 2MeSADP against H_2O_2 (Fig. 7B). Na_3VO_4 alone did not affect the cell viability of the astrocytes (light gray column). Additionally, Na_3VO_4 also reversed the inhibition by ATP or 2MeSADP of the H_2O_2-evoked phosphorylation of ERK1/2 in astrocytes (Fig. 7C). Then, we studied the effect of the selective $P2Y_1$ receptor antagonist MRS2179 (10 μM) on the PTP activity. H_2O_2 decreased the PTP activity to about one half. 2MeSADP restored the PTP activity and this effect was reversed by MRS2179 [Fig. 7D(1)]. As previously reported, $P2Y_1$ receptor activation also upregulates oxidoreductases such as TrxR, thereby protecting astrocytes against H_2O_2 (Shinozaki et al., 2005). The TrxR inhibitor auranofin (1 μM) also reversed the 2MeSADP-restored PTP activity. Furthermore, the thiol-containing antioxidant *N*-acetyl cystein (NAC, 10 mM) restored the H_2O_2-decreased PTP activity. In addition, we studied the effect of 2MeSADP, MRS2179 (10 μM), auranofin (1 μM), and NAC (10 mM) on the H_2O_2-evoked ERK1/2 activation [Fig. 7D(2)]. The inhibition of P-ERK1/2 activation by 2MeSADP (1 μM) was reversed by MRS2179 (10 μM) and auranofin (1 μM). In contrast, the H_2O_2-evoked ERK1/2 activation was prevented by NAC (10 mM). MRS2179 was added to the cells 1 h before the 2MeSADP treatment. Auranofin and NAC were added to the cells 1 h before H_2O_2 stimulation.

Involvement of src Tyrosine Kinase Family on H_2O_2-Evoked Cell Death and ERK1/2 Activation

Using Western blotting analysis, we studied whether H_2O_2 induces protein tyrosine phosphorylation. H_2O_2 evoked protein tyrosine phosphorylation, which was inhibited by pretreatment with ATP (100 μM, 24 h) or 2MeSADP (1 μM, 24 h) (Fig. 8A). This ATP- and

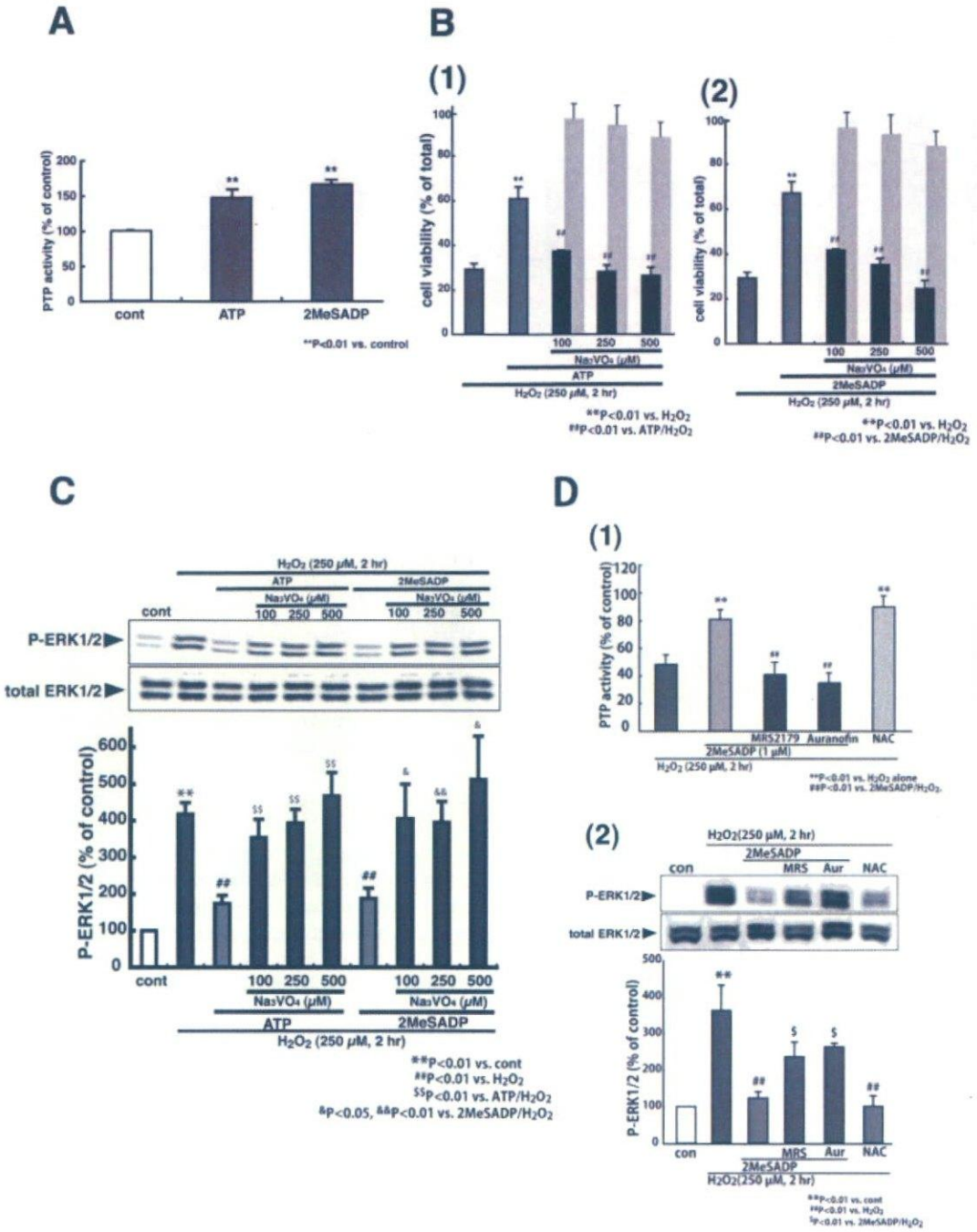

Fig. 7. The effect of ATP-induced PTP upregulation on H_2O_2-evoked cell death and ERK1/2 activation. **A**: ATP- and 2MeSADP-induced an increase of the PTP activity. ATP (100 μM, 24 h) and 2MeSADP (1 μM, 24 h) significantly increased the PTP activity (ATP: 148.3% ± 8.8%; 2MeSADP: 168.8% ± 4.8%, vs. control). Asterisks show significant difference from control ($^{**}P < 0.01$ vs. control, Student's *t*-test). **B**: PTP participates in ATP- and 2MeSADP-induced cytoprotective effect. The PTP inhibitor Na_3VO_4 (100–500 μM, 1 h) reversed the ATP(100 μM, 24 h)- and 2MeSADP(1 μM, 24 h)-induced protective effect concentration-dependently (black column). Na_3VO_4 alone did not affect the cell viability of the astrocytes (light gray column). Asterisks show significant difference from the response evoked by H_2O_2 ($^{**}P < 0.01$ vs. 250 μM H_2O_2, Student's *t*-test). Sharps show significant difference from the response by ATP/H_2O_2 or 2MeSADP/H_2O_2 ($^{\#\#}P < 0.01$ vs. ATP/H_2O_2 or 2MeSADP/H_2O_2, Student's *t*-test). **C**: PTP participates in ATP- and 2MeSADP-induced inhibition of H_2O_2-evoked ERK1/2 activation. Na_3VO_4 (100–500 μM, 1 h) reversed the ATP(100 μM, 24 h)- and 2MeSADP(1 μM, 24 h)-induced inhibition of H_2O_2-evoked ERK1/2 activation. The cells were treated with ATP and 2MeSADP 24 h before and during H_2O_2 treatment. Na_3VO_4 was added to the cells 1 h before the H_2O_2 (250 μM) treatment. Asterisks show significant difference from control ($^{**}P < 0.01$ vs. control, Student's *t*-test). Sharps show significant difference from H_2O_2 ($^{\#\#}P < 0.01$ vs. H_2O_2, Student's *t*-test). Dollar marks show significant difference from ATP/H_2O_2 or 2MeSADP/H_2O_2 ($^{\$}P < 0.05$, $^{\$\$}P < 0.01$ vs. ATP/H_2O_2 or 2MeSADP/H_2O_2, Student's *t*-test). **D**: The effect of MRS2179, auranofin, and NAC on PTP and ERK1/2 activity. (1) 2MeSADP (1 μM) restored the H_2O_2 (250 μM, 2 h)-decreased PTP activity and the effect was reversed by MRS2179 (10 μM) and auranofin (1 μM). NAC (10 mM) restored the PTP activity decreased by H_2O_2. Asterisks show significant difference from the response evoked by H_2O_2 ($^{**}P < 0.01$ vs. 250 μM H_2O_2, Student's *t*-test). Sharps show significant difference from the response by 2MeSADP/H_2O_2 ($^{\#\#}P < 0.01$ vs. 2MeSADP/H_2O_2). (2) The effect of MRS2179, auranofin, and NAC on H_2O_2-evoked ERK1/2 activation. MRS2179 (10 μM) and auranofin (1 μM) reversed the ERK1/2 activity inhibited by 2MeSADP. NAC (10 mM) prevented the H_2O_2-evoked ERK1/2 activation. Asterisks show significant difference from control ($^{**}P < 0.01$ vs. control, Student's *t*-test). Sharps show significant difference from H_2O_2 ($^{\#\#}P < 0.01$ vs. H_2O_2, Student's *t*-test). Dollar marks show significant difference from 2MeSADP/H_2O_2 ($^{\$}P < 0.05$ vs. 2MeSADP/H_2O_2, Student's Results were expressed as means *t*-test). Results were expressed as means ± SEM of triplicate measurements ($n = 3$).

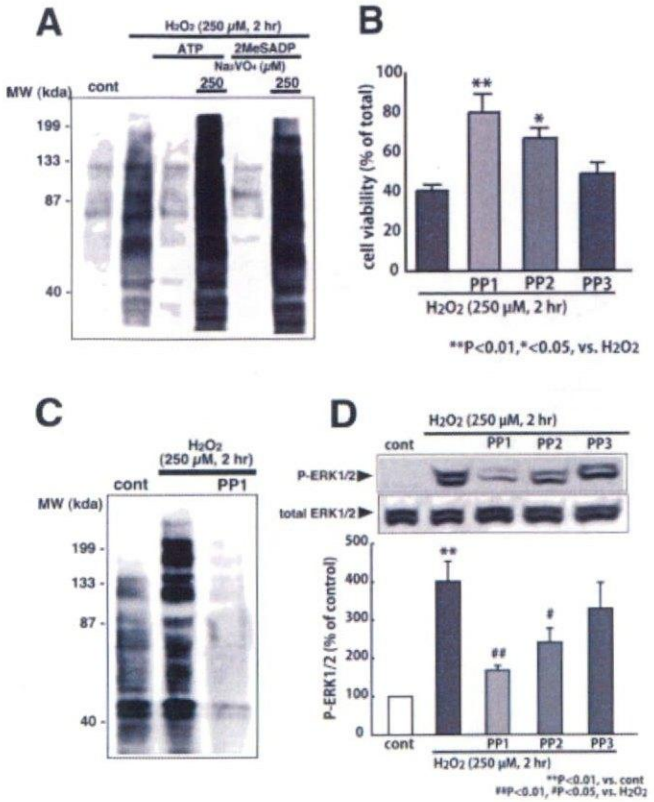

Fig. 8. The effects of the src family on the H_2O_2-evoked cell death and ERK1/2 activation. **A**: ATP and 2MeSADP prevented the H_2O_2-evoked protein tyrosine phosphorylation via PTP upregulation. H_2O_2 (250 μM) evoked the protein tyrosine phosphorylation. Na_3VO_4 (250 μM) markedly inhibited the ATP-(100 μM, 24 h) and 2MeSADP (1 μM, 24 h)-induced prevention of the H_2O_2-evoked protein tyrosine phosphorylation. Na_3VO_4 was applied to the cells 1 h before and during the H_2O_2 treatment. **B**: The effect of selective src family inhibitors on the H_2O_2-evoked cell death. PP1 and PP2 (250 nM) prevented the H_2O_2-evoked cell death but PP3 (250 nM) did not. Asterisks show significant difference from the response evoked by H_2O_2 ($^*P < 0.05$, $^{**}P < 0.01$ vs. 250 μM H_2O_2, Student's *t*-test) . **C**: The effect of PP1 on H_2O_2-evoked protein tyrosine phosphorylation. PP1 (250 nM) strongly inhibited the H_2O_2-evoked protein tyrosine phosphorylation. **D**: The effect of selective src family inhibitors on H_2O_2-evoked ERK1/2 activation. PP1 and PP2 (250 nM) inhibited H_2O_2-evoked ERK1/2 activation but PP3 (250 nM) did not. PP1, PP2, and PP3 were applied to the cells 1 h before and during the H_2O_2 treatment. Asterisks show significant difference from control ($^{**}P < 0.01$ vs. control, Student's *t*-test). Sharps show significant difference from H_2O_2 ($^{\#\#}P < 0.01$ vs. H_2O_2, Student's *t*-test). Results were expressed as means ± SEM of triplicate measurements ($n = 3$).

2MeSADP-induced prevention disappeared when the astrocytes were treated with Na_3VO_4 to inhibit the PTP activity, suggesting that ATP and 2MeSADP would inhibit tyrosine phosphorylation through a pathway(s) mediated by PTP. As it has been reported that H_2O_2 especially activates the src tyrosine kinase family of PTK (Lee and Esselman, 2002; Nishida et al., 2000), we pharmacologically studied whether the src family participates in the H_2O_2-evoked cell death and ERK1/2 activation. When the selective src family inhibitors PP1 (250 nM) and PP2 (250 nM) (Hanke et al., 1996) were added to the cells 1 h before H_2O_2 treatment, the H_2O_2-evoked cell death in astrocytes was abolished (Fig. 8B). The inactive analogue PP3 (250 nM) did not inhibit the H_2O_2-evoked cell death. PP1 (250 nM) also inhibited the H_2O_2-evoked protein tyrosine phosphorylation (Fig. 8C). In addition, the H_2O_2-evoked ERK1/2 activation was inhibited by PP1 and PP2 (250 nM) but not by PP3 (Fig. 8D). PP1, PP2, and PP3 were added to the cells 1 h before H_2O_2 stimulation.

DISCUSSION

In the present study, we demonstrated that ERK1/2 and src family are important molecules that promote the H_2O_2-evoked astrocytic cell death, and that ATP upregulates PTP expression and its activity, thereby preventing the H_2O_2-evoked src family and following ERK1/2 activation, resulting in the protection of astrocytes against H_2O_2-evoked cell death.

We clearly showed that the H_2O_2-evoked activation of ERK1/2 and accumulation of P-ERK in nuclei were critical events that promote cell death in astrocytes. ATP itself, however, which exhibited a protective effect against H_2O_2 in our study, is also known to activate ERK1/2 in astrocytes (Neary et al., 1999, 2003; Panenka et al., 2001). In fact, ATP and 2MeSADP activated ERK1/2 in astrocytes. However, the ERK1/2 activation by ATP, in contrast to that by H_2O_2, was transient (5–15 min after stimulation) and did not affect the astrocyte cell viability. Furthermore, 2MeSADP-activated ERK1/2 seems to function rather as an essential signal that prevents cell death and induces the upregulation of oxidoreductases and PTP gene expression. Thus, such a discrepancy appears to result from spatio- and temporal-behavioral differences of P-ERK1/2. It is known that, after faint brain ischemia, neuronal cells acquire tolerance to a subsequent more serious ischemic injury (Chen and Simon, 1997; Dawson and Dawson, 2000; Schaller and Graf, 2002). The similarity between such preconditioning against ischemia and the preconditioning of ERK1/2 against H_2O_2-evoked cell death is very interesting.

In the present study, the extent of the ERK1/2 activity appeared to be important in the H_2O_2-evoked cell death because of the correspondence between the concentration-dependency of the H_2O_2-evoked ERK1/2 activity and that of the H_2O_2-evoked cell death (Shinozaki et al., 2005). Although recent studies also have reported that H_2O_2-activated ERK1/2 evokes cell death in glioma and osteoblastic cells (Choi et al., 2005; Levinthal and Defranco, 2005), the spatio- and temporal behavior of P-ERK1/2 remained unclear. P-ERK1/2 is known to translocate into the nucleus (Rosenberger et al., 2001) and accumulate there (Brand et al., 2001; Stanciu and DeFranco, 2002), thereby inducing neuronal death. In the immunocytochemical analysis, stimulation by 250 μM but not by 50 μM H_2O_2 for 2 h induced P-ERK1/2 accumulation in the nucleus. Most of the total ERK1/2 existed in the cytoplasm and was not affected by H_2O_2 (50 or 250 μM). Accordingly, it is conceivable that only P-ERK1/2, activated by high concentrations (i.e. 250 μM) of H_2O_2, accumulates in the nucleus and induces cell

death. In a spatiotemporal analysis of P-ERK1/2, although there was a time-dependent activation of ERK1/2 by 50 and 250 μM H_2O_2 at the whole cell level, the fraction of N = E was increased transiently (~15 min after stimulation) by 50 μM H_2O_2 but time-dependently by 250 μM. These results suggest that the long-term accumulation of P-ERK1/2 into the nucleus participates in the H_2O_2-evoked cell death.

In physiological conditions, it is suggested that the P-ERK1/2 translocated into the nucleus is dephosphorylated by MAPK phosphatase (MAPKP), especially by the ERK1/2 selective phosphatase MAPK phosphatase-3 (MKP-3) (Dowd et al., 1998; Groom et al., 1996) and is exported from the nucleus depending on MKP-3 (Karlsson et al., 2004). The interaction between MKP-3 and ERK1/2 requires arginine residues of MKP-3 (Nichols et al., 2000). Because many amino acids, including arginines, in protein are oxidized by H_2O_2 (Amici et al., 1989; Moskovitz et al., 2002; Stadtman and Berlett, 1997; Taborsky, 1973), the interaction of MKP-3 and ERK1/2 and the nuclear export of ERK1/2 may be affected by H_2O_2. Furthermore, the ERK1/2 inactivating enzyme MAPKP is inactivated by H_2O_2 (Foley et al., 2004; Levinthal and Defranco, 2005). In conditions with oxidative stress, it is conceivable that the dephosphorylation and nuclear export of activated-ERK1/2 are attenuated because of the decreased MAPKP function and the association between MAPKP and ERK1/2, which thereby induces the prolonged activation and nuclear accumulation of ERK1/2.

With regard to the upstream molecule that activates ERK1/2 in response to H_2O_2, we found that the src family is important. Furthermore, we demonstrated that activation of $P2Y_1$ receptors inhibits the activation of src family and subsequent signaling cascades by upregulating the PTP expression and activity. We previously reported that ATP upregulates the thiol-containing protein TrxR (Shinozaki et al., 2005). The enzymatic activity of PTP requires reduction of the cystein residue in its active center (Cho et al., 2004; Persson et al., 2004). Accordingly, the redox state of the cystein residue in PTP is considered to crucially affect its phosphatase activity. The decreased activity of PTP in an oxidative state is recovered by adding thiol-containing protein such as glutathione (Salmeen et al., 2003) and thioredoxin (Lee and Esselman, 2002). In fact, the $P2Y_1$ receptor activation-induced restoration of the PTP activity was reversed by auranofin, indicating that TrxR restores the PTP activity. Additionally, the antioxidant NAC restored the PTP activity decreased by H_2O_2 (250 μM). The protective effect of PTP induced by ATP requires either an increase in the amount/activity of PTP or a reduction, in which the upregulated TxrR would have a critical role (Shinozaki et al., 2005). Furthermore, such ATP-induced oxidoreductases may preserve the MKP-3 activity, thereby enhancing the dephosphorylation and inactivation of ERK1/2 and the nuclear export of ERK1/2.

PTP and PTK regulate protein tyrosine phosphorylation in close coordination with each other. ATP prevented the H_2O_2-induced protein tyrosine phosphorylation by increasing the PTP activity. The inhibition of the H_2O_2-evoked cell death by PP1 and PP2 and the tyrosine phosphorylation by PP1 indicates that the src tyrosine kinase family is related to the H_2O_2-evoked cell death. Additionally, PP1 and PP2 inhibited the H_2O_2-evoked ERK1/2 activation, indicating that ERK1/2 is activated following src family activation. As the src family is activated by cystein oxidation independently of tyrosine phosphorylation (Akhand et al., 1999; Pu et al., 1996), under oxidative stress such as by H_2O_2 treatment or in condition of ischemia/reperfusion-injury, the src family could be activated independent of tyrosine phosphorylation. In contrast to src activation, PTP and MAPKP are inactivated by oxidation of the cystein residue under oxidative conditions (Cho et al., 2004; Foley et al., 2004; Meng et al., 2004). Briefly, the "irresponsive to control" signal transduction could be caused under oxidative conditions.

In conclusion, we clearly demonstrated that the src family activation followed by strong ERK1/2 activation and prolonged P-ERK1/2 accumulation into the nucleus participated in the H_2O_2-evoked cell death of astrocytes. ATP/$P2Y_1$ receptor activation inhibits H_2O_2-evoked ERK1/2 activation by preventing the H_2O_2-evoked src activation via upregulation of PTP expression/activity. Our present findings suggest that the gliotransmitter ATP protects astrocytes against oxidative stress by counteracting the intracellular signaling pathway that evokes cell death.

ACKNOWLEDGMENTS

We thank Tomoko Obama for technical assistance.

REFERENCES

Akhand AA, Pu M, Senga T, Kato M, Suzuki H, Miyata T, Hamaguchi M, Nakashima I. 1999. Nitric oxide controls src kinase activity through a sulfhydryl group modification-mediated Tyr-527-independent and Tyr-416-linked mechanism. J Biol Chem 274:25821–25826.

Alessandrini A, Namura S, Moskowitz MA, Bonventre JV. 1999. MEK1 protein kinase inhibition protects against damage resulting from focal cerebral ischemia. Proc Natl Acad Sci USA 96:12866–12869.

Alessi DR, Cuenda A, Cohen P, Dudley DT, Saltiel AR. 1995. PD 098059 is a specific inhibitor of the activation of mitogen-activated protein kinase kinase in vitro and in vivo. J Biol Chem 270:27489–27494.

Amici A, Levine RL, Tsai L, Stadtman ER. 1989. Conversion of amino acid residues in proteins and amino acid homopolymers to carbonyl derivatives by metal-catalyzed oxidation reactions. J Biol Chem 264:3341–3346.

Bennett BL, Sasaki DT, Murray BW, O'Leary EC, Sakata ST, Xu W, Leisten JC, Motiwala A, Pierce S, Satoh Y, Bhagwat SS, Manning AM, Anderson DW. 2001. SP600125, an anthrapyrazolone inhibitor of Jun N-terminal kinase. Proc Natl Acad Sci USA 98:13681–13686.

Boschert U, Muda M, Camps M, Dickinson R, Arkinstall S. 1997. Induction of the dual specificity phosphatase PAC1 in rat brain following seizure activity. Neuroreport 8:3077–3080.

Boulton TG, Nye SH, Robbins DJ, Ip NY, Radziejewska E, Morgenbesser SD, DePinho RA, Panayotatos N, Cobb MH, Yancopoulos GD. 1991. ERKs: A family of protein-serine/threonine kinases that are activated and tyrosine phosphorylated in response to insulin and NGF. Cell 65:663–675.

Brand A, Gil S, Seger R, Yavin E. 2001. Lipid constituents in oligodendroglial cells alter susceptibility to H_2O_2-induced apoptotic cell death via ERK activation. J Neurochem 76:910–918.

Brugge JS, Cotton PC, Queral AE, Barrett JN, Nonner D, Keane RW. 1985. Neurones express high levels of a structurally modified, activated form of pp60c-src. Nature 316:554–557.

Chen J, Simon R. 1997. Ischemic tolerance in the brain. Neurology 48:306–311.

Chen RH, Sarnecki C, Blenis J. 1992. Nuclear localization and regulation of erk- and rsk-encoded protein kinases. Mol Cell Biol 12:915–927.

Cho SH, Lee CH, Ahn Y, Kim H, Ahn CY, Yang KS, Lee SR. 2004. Redox regulation of PTEN and protein tyrosine phosphatases in H_2O_2-mediated cell signaling. FEBS Lett 560(1–3):7–13.

Choi JS, Park HJ, Kim HY, Kim SY, Lee JE, Choi YS, Chun MH, Chung JW, Lee MY. 2005. Phosphorylation of PTEN and Akt in astrocytes of the rat hippocampus following transient forebrain ischemia. Cell Tissue Res 319:359–366.

Dawson VL, Dawson TM. 2000. Neuronal ischaemic preconditioning. Trends Pharmacol Sci 21:423–424.

Dowd S, Sneddon AA, Keyse SM. 1998. Isolation of the human genes encoding the pyst1 and Pyst2 phosphatases: Characterisation of Pyst2 as a cytosolic dual-specificity MAP kinase phosphatase and its catalytic activation by both MAP, SAP kinases. J Cell Sci 111(Part 22):3389–3399.

Fam SR, Gallagher CJ, Salter MW. 2000. P2Y(1) purinoceptor-mediated Ca(2+) signaling and Ca(2+) wave propagation in dorsal spinal cord astrocytes. J Neurosci 20:2800–2808.

Favata MF, Horiuchi KY, Manos EJ, Daulerio AJ, Stradley DA, Feeser WS, Van Dyk DE, Pitts WJ, Earl RA, Hobbs F, Copeland RA, Magolda RL.Scherle PA, Trzaskos JM. 1998. Identification of a novel inhibitor of mitogen-activated protein kinase kinase. J Biol Chem 273:18623–18632.

Fialkow L, Chan CK, Rotin D, Grinstein S, Downey GP. 1994. Activation of the mitogen-activated protein kinase signaling pathway in neutrophils. Role of oxidants. J Biol Chem 269:31234–31242.

Fields RD, Stevens-Graham B. 2002. New insights into neuron-glia communication. Science 298:556–562.

Foley TD, Armstrong JJ, Kupchak BR. 2004. Identification and H_2O_2 sensitivity of the major constitutive MAPK phosphatase from rat brain. Biochem Biophys Res Commun 315:568–574.

Gonzalez FA, Seth A, Raden DL, Bowman DS, Fay FS, Davis RJ. 1993. Serum-induced translocation of mitogen-activated protein kinase to the cell surface ruffling membrane and the nucleus. J Cell Biol 122:1089–1101.

Groom LA, Sneddon AA, Alessi DR, Dowd S, Keyse SM. 1996. Differential regulation of the MAP, SAP and RK/p38 kinases by Pyst1, a novel cytosolic dual-specificity phosphatase. EMBO J 15:3621–3632.

Guo J, Meng F, Zhang G, Zhang Q. 2003. Free radicals are involved in continuous activation of nonreceptor tyrosine protein kinase c-Src after ischemia/reperfusion in rat hippocampus. Neurosci Lett 345:101–104.

Guyton KZ, Liu Y, Gorospe M, Xu Q, Holbrook NJ. 1996. Activation of mitogen-activated protein kinase by H_2O_2. Role in cell survival following oxidant injury. J Biol Chem 271:4138–4142.

Hanke JH, Gardner JP, Dow RL, Changelian PS, Brissette WH, Weringer EJ, Pollok BA, Connelly PA. 1996. Discovery of a novel, potent, and Src family-selective tyrosine kinase inhibitor. Study of Lck- and FynT-dependent T cell activation. J Biol Chem 271:695–701.

Hansson E, Ronnback L. 2003. Glial neuronal signaling in the central nervous system. FASEB J 17:341–348.

Heffetz D, Bushkin I, Dror R, Zick Y. 1990. The insulinomimetic agents H_2O_2 and vanadate stimulate protein tyrosine phosphorylation in intact cells. J Biol Chem 265:2896–2902.

Inoue K. 2002. Microglial activation by purines and pyrimidines. Glia 40:156–163.

Karlsson M, Mathers J, Dickinson RJ, Mandl M, Keyse SM. 2004. Both nuclear-cytoplasmic shuttling of the dual specificity phosphatase MKP-3 and its ability to anchor MAP kinase in the cytoplasm are mediated by a conserved nuclear export signal. J Biol Chem 279:41882–41891.

Kimura M, Maeda K, Hayashi S. 1992. Cytosolic calcium increase in coronary endothelial cells after H_2O_2 exposure and the inhibitory effect of U78517F. Br J Pharmacol 107:488–493.

Konishi H, Matsuzaki H, Takaishi H, Yamamoto T, Fukunaga M, Ono Y, Kikkawa U. 1999. Opposing effects of protein kinase C δ and protein kinase B α on H_2O_2-induced apoptosis in CHO cells. Biochem Biophys Res Commun 264:840–846.

Lee K, Esselman WJ. 2002. Inhibition of PTPs by H_2O_2 regulates the activation of distinct MAPK pathways. Free Radic Biol Med 33:1121–1132.

Levinthal DJ, Defranco DB. 2005. Reversible oxidation of ERK-directed protein phosphatases drives oxidative toxicity in neurons. J Biol Chem 280:5875–5883.

Marshall CJ. 1995. Specificity of receptor tyrosine kinase signaling: Transient versus sustained extracellular signal-regulated kinase activation. Cell 80:179–185.

McLaughlin MM, Kumar S, McDonnell PC, Van Horn S, Lee JC, Livi GP, Young PR. 1996. Identification of mitogen-activated protein (MAP) kinase-activated protein kinase-3, a novel substrate of CSBP p38 MAP kinase. J Biol Chem 271:8488–8492.

Meng TC, Buckley DA, Galic S, Tiganis T, Tonks NK. 2004. Regulation of insulin signaling through reversible oxidation of the protein-tyrosine phosphatases TC45 and PTP1B. J Biol Chem 279:37716–37725.

Moskovitz J, Yim MB, Chock PB. 2002. Free radicals and disease. Arch Biochem Biophys 397:354–359.

Murray B, Alessandrini A, Cole AJ, Yee AG, Furshpan EJ. 1998. Inhibition of the p44/42 MAP kinase pathway protects hippocampal neurons in a cell-culture model of seizure activity. Proc Natl Acad Sci USA 95:11975–11980.

Namura S, Iihara K, Takami S, Nagata I, Kikuchi H, Matsushita K, Moskowitz MA, Bonventre JV, Alessandrini A. 2001. Intravenous administration of MEK inhibitor U0126 affords brain protection against forebrain ischemia and focal cerebral ischemia. Proc Natl Acad Sci USA 98:11569–11574.

Neary JT, Kang Y, Bu Y, Yu E, Akong K, Peters CM. 1999. Mitogenic signaling by ATP/P2Y purinergic receptors in astrocytes: Involvement of a calcium-independent protein kinase C, extracellular signal-regulated protein kinase pathway distinct from the phosphatidylinositol-specific phospholipase C/calcium pathway. J Neurosci 19:4211–4220.

Neary JT, Kang Y, Willoughby KA, Ellis EF. 2003. Activation of extracellular signal-regulated kinase by stretch-induced injury in astrocytes involves extracellular ATP, P2 purinergic receptors. J Neurosci 23:2348–2356.

Nichols A, Camps M, Gillieron C, Chabert C, Brunet A, Wilsbacher J, Cobb M, Pouyssegur J, Shaw JP, Arkinstall S. 2000. Substrate recognition domains within extracellular signal-regulated kinase mediate binding and catalytic activation of mitogen-activated protein kinase phosphatase-3. J Biol Chem 275:24613–24621.

Nishida M, Maruyama Y, Tanaka R, Kontani K, Nagao T, Kurose H. 2000. G α(i) and G α(o) are target proteins of reactive oxygen species. Nature 408:492–495.

Ohtsuki T, Matsumoto M, Kitagawa K, Mabuchi T, Mandai K, Matsushita K, Kuwabara K, Tagaya M, Ogawa S, Ueda H, Kamada T, Yanagihara T. 1996. Delayed neuronal death in ischemic hippocampus involves stimulation of protein tyrosine phosphorylation. Am J Physiol 271(4, Part 1):C1085–C1097.

Oppenheim RW. 1991. Cell death during development of the nervous system. Annu Rev Neurosci 14:453–501.

Panenka W, Jijon H, Herx LM, Armstrong JN, Feighan D, Wei T, Yong VW, Ransohoff RM, MacVicar BA. 2001. P2X7-like receptor activation in astrocytes increases chemokine monocyte chemoattractant protein-1 expression via mitogen-activated protein kinase. J Neurosci 21:7135–7142.

Persson C, Sjoblom T, Groen A, Kappert K, Engstrom U, Hellman U, Heldin CH, den Hertog J, Ostman A. 2004. Preferential oxidation of the second phosphatase domain of receptor-like PTP-α revealed by an antibody against oxidized protein tyrosine phosphatases. Proc Natl Acad Sci USA 101:1886–1891.

Pu M, Akhand AA, Kato M, Hamaguchi M, Koike T, Iwata H, Sabe H, Suzuki H, Nakashima I. 1996. Evidence of a novel redox-linked activation mechanism for the Src kinase which is independent of tyrosine 527-mediated regulation. Oncogene 13:2615–2622.

Rosenberger J, Petrovics G, Buzas B. 2001. Oxidative stress induces proorphanin FQ, proenkephalin gene expression in astrocytes through p38- and ERK-MAP kinases and NF-κB. J Neurochem 79:35–44.

Salmeen A, Andersen JN, Myers MP, Meng TC, Hinks JA, Tonks NK, Barford D. 2003. Redox regulation of protein tyrosine phosphatase 1B involves a sulphenyl-amide intermediate. Nature 423:769–773.

Schaller B, Graf R. 2002. Cerebral ischemic preconditioning. An experimental phenomenon or a clinical important entity of stroke prevention? J Neurol 249:1503–1511.

Segal RA, Greenberg ME. 1996. Intracellular signaling pathways activated by neurotrophic factors. Annu Rev Neurosci 19:463–489.

Shinozaki Y, Koizumi S, Ishida S, Sawada JI, Ohno Y, Inoue K. 2005. Cytoprotection against oxidative stress-induced damage of astrocytes by extracellular ATP via P2Y(1) receptors. Glia 49:288–300.

Shisheva A, Shechter Y. 1993. Role of cytosolic tyrosine kinase in mediating insulin-like actions of vanadate in rat adipocytes. J Biol Chem 268:6463–6469.

Stadtman ER, Berlett BS. 1997. Reactive oxygen-mediated protein oxidation in aging and disease. Chem Res Toxicol 10:485–494.

Stanciu M, DeFranco DB. 2002. Prolonged nuclear retention of activated extracellular signal-regulated protein kinase promotes cell death generated by oxidative toxicity or proteasome inhibition in a neuronal cell line. J Biol Chem 277:4010–4017.

Subramaniam S, Zirrgiebel U, Von Bohlen Und Halbach O, Strelau J, Laliberte C, Kaplan DR, Unsicker K. 2004. ERK activation promotes neuronal degeneration predominantly through plasma membrane damage and independently of caspase-3. J Cell Biol 165:357–369.

Sugrue MM, Brugge JS, Marshak DR, Greengard P, Gustafson EL. 1990. Immunocytochemical localization of the neuron-specific form of the c-src gene product, pp60c-src(+), in rat brain. J Neurosci 10:2513–2527.

Taborsky G. 1973. Oxidative modification of proteins in the presence of ferrous ion and air. Effect of ionic constituents of the reaction medium on the nature of the oxidation products. Biochemistry 12:1341–1348.

Takahashi M, Berk BC. 1996. Mitogen-activated protein kinase (ERK1/2) activation by shear stress and adhesion in endothelial cells. Essential role for a herbimycin-sensitive kinase. J Clin Invest 98:2623–2631.

Takano S, Fukuyama H, Fukumoto M, Kimura J, Xue JH, Ohashi H, Fujita J. 1996. PRL-1, a protein tyrosine phosphatase, is expressed in neurons and oligodendrocytes in the brain and induced in the cerebral cortex following transient forebrain ischemia. Brain Res Mol Brain Res 40:105–115.

Tan J, Town T, Mori T, Wu Y, Saxe M, Crawford F, Mullan M. 2000. CD45 opposes β-amyloid peptide-induced microglial activation via inhibition of p44/42 mitogen-activated protein kinase. J Neurosci 20:7587–7594.

Ushio-Fukai M, Alexander RW, Akers M, Yin Q, Fujio Y, Walsh K, Griendling KK. 1999. Reactive oxygen species mediate the activation of Akt/protein kinase B by angiotensin II in vascular smooth muscle cells. J Biol Chem 274:22699–22704.

Wang X, Martindale JL, Liu Y, Holbrook NJ. 1998. The cellular response to oxidative stress: Influences of mitogen-activated protein kinase signalling pathways on cell survival. Biochem J 333(Part 2):291–300.

Xia Z, Dickens M, Raingeaud J, Davis RJ, Greenberg ME. 1995. Opposing effects of ERK, JNK-p38 MAP kinases on apoptosis. Science 270:1326–1331.

Yu XM, Salter MW. 1999. Src, a molecular switch governing gain control of synaptic transmission mediated by *N*-methyl-D-aspartate receptors. Proc Natl Acad Sci USA 96:7697–7704.

Journal of Neuroscience Research 83:1461–1470 (2006)

Microglial α7 Nicotinic Acetylcholine Receptors Drive a Phospholipase C/IP_3 Pathway and Modulate the Cell Activation Toward a Neuroprotective Role

Tomohisa Suzuki,[1] Izumi Hide,[1]* Akiyo Matsubara,[1] Chihiro Hama,[1] Kana Harada,[1] Kanako Miyano,[1] Matthias Andrä,[2] Hiroaki Matsubayashi,[2] Norio Sakai,[2] Shinichi Kohsaka,[3] Kazuhide Inoue,[4] and Yoshihiro Nakata[1]

[1]Department of Pharmacology, Graduate School of Biomedical Sciences, Hiroshima University, Hiroshima, Japan
[2]Department of Molecular and Pharmacological Neuroscience, Graduate School of Biomedical Sciences, Hiroshima University, Hiroshima, Japan
[3]Department of Neurochemistry, National Institute of Neuroscience, Tokyo, Japan
[4]Department of Molecular and System Pharmacology, Graduate School of Pharmaceutical Sciences, Kyushu University, Fukuoka, Japan

Microglia perform both neuroprotective and neurotoxic functions in the brain, with this depending on their state of activation and their release of mediators. Upon $P2X_7$ receptor stimulation, for example, microglia release small amounts of TNF, which protect neurons, whereas LPS causes massive TNF release leading to neuroinflammation. Here we report that, in rat primary cultured microglia, nicotine enhances $P2X_7$ receptor-mediated TNF release, whilst suppressing LPS-induced TNF release but without affecting TNF mRNA expression via activation of α7 nicotinic acetylcholine receptors (α7 nAChRs). In microglia, nicotine elicited a transient increase in intracellular Ca^{2+} levels, which was abolished by specific blockers of α7 nAChRs. However, this response was independent of extracellular Ca^{2+} and blocked by U73122, an inhibitor of phospholipase C (PLC), and xestospongin C, a blocker of the IP_3 receptor. Repeated experiments showed that currents were not detected in nicotine-stimulated microglia. Moreover, nicotine modulation of LPS-induced TNF release was also blocked by xestospongin C. Upon LPS stimulation, inhibition of TNF release by nicotine was associated with the suppression of JNK and p38 MAP kinase activation, which regulate the post-transcriptional steps of TNF synthesis. In contrast, nicotine did not alter any MAP kinase activation, but enhanced Ca^{2+} response in $P2X_7$ receptor-activated microglia. In conclusion, microglial α7 nAChRs might drive a signaling process involving the activation of PLC and Ca^{2+} release from intracellular Ca^{2+} stores, rather than function as conventional ion channels. This novel α7 nAChR signal may be involved in the nicotine modification of microglia activation towards a neuroprotective role by suppressing the inflammatory state and strengthening the protective function.

Key words: microglia; nicotinic acethylcholine receptor; ATP; lipopolysaccharide; tumor necrosis factor

Nicotinic acetylcholine receptors (nAChRs) contribute to brain functions such as the modulation of synaptic transmission, memory formation, and neuroprotection (MacxDermot et al., 1999; Cordero-Erausquin et al., 2000; Laudenbach et al., 2002; Daijas-Bailador and Wonnacott, 2004). Among nAChRs, α7 and α4β2 are the most abundant subunits in the brain (Buisson and Bertrand, 2002). The α7 nAChRs are ion channels forming homo-pentamers with high Ca^{2+} permeability, which exhibit a low affinity for acetylcholine (ACh) and nicotine and are desensitized rapidly. In contrast, α4β2 nAChRs are considered to exhibit a highly affinity for ACh and nicotine and are desensitized slowly (Cordero-Erausquin et al., 2000). Although these nAChRs have been regarded to be expressed mainly in neuronal cells, recent evidence suggests that the α7 nAChRs also function in nonexcitable cells, such as endothelial cells, keratinocytes, and T cells (Sharma and Vijayaraghavan, 2002).

Microglia are the primary immune cells in the central nervous system (CNS). Under pathological conditions such as brain damage and stroke, they are rapidly activated, phagocytose dead cells, and secrete various cytokines, including tumor necrosis factor (TNF), interleukin-1β

Contract grant sponsor: The Japanese Ministry of Education, Culture, Sports, Science and Technology; Contract grant sponsor: The Japanese Smoking Research Association.

*Correspondence to: Izumi Hide, Department of Pharmacology, Graduate School of Biomedical Sciences, Hiroshima University, 1-2-3 Kasumi, Minami-ku, Hiroshima 734-8553, Japan.
E-mail: ihide@hiroshima-u.ac.jp

Received 2 August 2005; Revised 16 January 2006; Accepted 16 February 2006

Published online 1 May 2006 in Wiley InterScience (www.interscience.wiley.com). DOI: 10.1002/jnr.20850

(IL-1β), and IL-6 (Aliosi, 2001; Shigemoto-Mogami et al., 2002). TNF, a proinflammatory and cytotrophic cytokine up-regulated in the brain in response to various insults or injury (Barone et al., 1997; Shohami et al., 1999), is released mainly by microglia and astrocytes around the injured area. Lipopolysaccharide (LPS), one of the main components of gram (–) bacterial outer membranes, induces the release of large amounts of TNF from macrophages and microglia, leading to inflammation and possibly neuronal destruction (Kim et al., 2000). Microglia also release moderate amounts of TNF in response to extracellular ATP via activation of the ionotrophic $P2X_7$ receptor (Hide et al., 2000; Suzuki et al., 2004). This manner of TNF release protects neurons against glutamate cytotoxicity (Suzuki et al., 2004).

Recently, it was revealed that α7 nAChRs are expressed in mouse brain microglia and are involved in the suppression of neuroinflammation (Shytle et al., 2004). In this study, we found that, in rat primary cultured microglia, the activation of α7 nAChRs by nicotine enhanced protective TNF release induced by ATP stimulation, in addition to having a suppressive effect on LPS-induced TNF release via α7 nAChRs. Furthermore, the present results demonstrate that these microglial α7 nAChRs have different properties from conventional neuronal α7 nAChRs, not functioning as ion channels but coupling to phospholipase C (PLC) activation and Ca^{2+} mobilization from IP_3-sensitive Ca^{2+} stores. We also investigated the signaling mechanism by which α7 nAChR activation could modulate TNF release in response to LPS (TLR4 activation) and ATP or BzATP ($P2X_7$ receptor activation).

MATERIALS AND METHODS

Reagents

Reagents were obtained from the following sources: all reagents for cell culture, (–)nicotine hydrogen tartrate, LPS, ATP, 2′- and 3′-O-(benzoyl-benzoyl) adenosine 5′-triphosphate (BzATP), α-bungarotoxin, methyllycaconitine, and xestospongin C were from Sigma Chemical Co. (St. Louis, MO); U73122 from Calbiochem (San Diego, CA); BAPTA-AM from WAKO Pure Chemical Industries (Osaka, Japan); rat TNF ELISA kit from Biosource International (Camarillo, CA); polyclonal antibody against α7 nAChRs from Santa Cruz Biotechnology (Santa Cruz, CA); antibody kits for p42/p44 (ERK), JNK, and p38 MAP kinase from Cell Signaling Technology (Beverly, MA). All other reagents were purchased from commercial sources and were of the highest available purity.

Cell Culture

Microglia were obtained from the primary cell cultures of neonatal rat brains as previously described (Nakajima et al., 1992). After 7–16 days in culture, microglia were prepared as a floating cell suspension. Aliquots ($1.5–2.0 \times 10^5$ cells) were transferred to the wells of a 24-well plate and allowed to adhere at 37°C for 45 min. Unattached cells were removed by rinsing with serum-free Dulbecco's modified Eagle's medium (DMEM).

TNF Assay

Microglia were incubated with 0.4 ml of serum-free DMEM with or without drugs for 3 hr. TNF was assayed in 50-μl samples by using a rat TNF ELISA kit according to the manufacturer's instructions.

Isolation of Total RNA, RT-PCR, and Real-Time Quantitative RT-PCR

Total RNA was isolated from microglia with Trizol reagent (Life Technologies, Inc.) according to the manufacturer's protocol. The amounts of tRNA was determined by using absorption of light at 260 and 280 nm.

The expression of mRNA of α7 nAChR subunit was detected by nested RT-PCR in rat microglia. RT-PCR was performed with an Access RT-PCR system (Promega, Madison, WI). Two sets of primers used to identify α7 were directed toward portions of exons 9–10: the first sets, forward, 5′-TCATGCTGCTTGTGGCTGAG-3′ and reverse sets, 5′-CCAATTCTCACCCTCCAGATTCTC-3′, and the second sets, forward, 5′-GCAACATCTGATTCTGTGCCCTTG-3′ and reverse, 5′-TCTGCGCATTTCCTACTTGA-3′. Thermocycling conditions were as follows: 95°C for 30 min; 45 cycles of 95°C for 15 sec, 60°C for 60 sec; PCR was performed in a tube with a total volume of 50 μl of reverse transcriptase mixture containing 1 mM $MgSO_4$, 0.2 mM dNTP, 0.1 U/μl Tfl DNA polymerase, 1 U/μl AMV RT.

The expression levels of mRNA for TNF were measured by real-time quantitative RT-PCR (ABI Prism model 7700 sequence detection system; PE Applied Biosystems, Foster City, CA) as described previously (Suzuki et al., 2004). RT-PCR was carried out by using TaqMan one-step RT-PCR Maser Mix reagents kit according to the manufacturer's protocol (Applied Biosystems). The sequences of the forward and reverse primers were 5′-ACAAGGCTGCCCCGACTAC-3′ and 5′-TCCTGGTATGAAATGGCAAACC-3′ respectively. The TaqMan fluorogenic probe was 5′-6FAM-TGCTCCTCACCCACACCGTCAGC-TAMIRA-3′. During PCR amplification, 5′ nucleotidase activity of AmpliTaq Gold DNA polymerase cleaves the TaqMan probe separating the 5′ reporter dye from the 3′ quencher dye, resulting in increased fluorescence of the reporter. The threshold cycle, C_T, which correlates inversely with the target mRNA levels, was measured as the cycle number at which reporter fluorescent emission increases above a threshold level. The TNF mRNA levels were corrected for the C_T values of glyceraldehydes-3-phosphate dehydrogenase (GAPDH) RNA by using VIC probe according to the manufacturer's protocol.

Measurement of Intracellular Ca^{2+} Concentration in Microglia

Microglia were plated on glass coverslips with a silicon rubber wall (Flexiperm; Heraeus Biotechnology, Hanau, Germany) at a density of 3×10^5 cells/well and maintained in 10% CO_2. After rinsing, the cells were loaded with 2.5 μM fura-2 acetoxymethyl ester for 20 min at room temperature. Fura-2-loaded cells were placed on a fluorescence-image microscope and stimulated by nicotine. The fura-2 fluorescence was measured with excitation at 340 and 380 nm and at

an emission wavelength of 510 nm. The video image output was digitized by an Argus 50 color image processor (Hamamatsu Photonics, Shizuoka, Japan) as described elsewhere (Hide et al., 1997).

Western Blot Analysis

Western blots were performed for the analysis of α7 nAChRs expression and for the analysis of ERK (p44/42), JNK, and p38 activation using each MAP kinase antibody. In brief, the cells were washed with phosphate-buffered saline, lysed by adding sodium dodecyl sulfate (SDS) sample buffer, and sonicated. After heating to 95°C for 5 min, the protein samples were separated by SDS-polyacrylamide gel electrophoresis (PAGE) and blotted onto polyvinylimide difluoride (PVDF) membranes. The membranes were blocked with blocking buffer containing 5% skim milk for 3 hr at room temperature and incubated with primary antibody with gentle agitation overnight at 4°C. After washing, the membranes were incubated for 1 hr at room temperature with horseradish peroxidase-conjugated secondary antibody and horseradish peroxidase-conjugated anti-biotin antibody to detect biotinylated protein markers. The membranes were then washed and incubated with Lumi GLO, and the proteins were detected by exposure to X-ray films.

Whole-Cell Patch Clamp

We performed whole-cell patch clamp for microglia according to the methods previously described (Matsubayashi et al., 2004). Microglia were transferred into a recording chamber, and the chamber was perfused continuously with external bath solution at 2 ml/min. The ionic composition of the external solution was as follows (in mM): NaCl, 165; KCl, 5; glucose, 10; $CaCl_2$, 2; HEPES, 5; and the pH of the solution was adjusted to 7.3 with NaOH. Experiments were carried out at room temperature. In voltage-clamp modes, drug-induced currents were recorded from microglia according to the standard whole-cell patch clamp technique by using an Axopatch 200A patch clamp system (Axon Instruments, Foster City, CA). Patch pipettes were pulled from borosilicate capillary glass (World Precision Instrument-Japan, o.d. 1.5 mm) and had resistances between 3 and 7 MΩ when filled with an internal solution with the following ionic composition (in mM): CsCl, 80; CsF, 80; $MgCl_2$, 2; HEPES, 10; Cs-EGTA, 10 (pH adjusted to 7.3 with CsOH). The series resistance of the patches was 10–25 MΩ and was not compensated. The signals of currents were filtered at 2 kHz and directly sampled by a microcomputer using the program pCLAMP (Axon Instruments). The drugs were delivered to the microglia from a pore 400 μm in diameter at the apex of a U-shaped tube ("U-tube") positioned about 50 μm directly above the target microglia. With this drug application system, the drug solution was ejected from the pore when the solenoid valve was closed electronically, and then the solution surrounding target microglia was quickly exchanged to drug solution at the desired concentrations. The whole-cell currents were recorded at −60 mV of holding potential.

Statistical Analysis

Statistical analysis of data was performed via one-way ANOVA and Dunnett's test.

RESULTS

Nicotine Inhibits LPS-Induced TNF Release but Enhances ATP- or BzATP-Induced TNF Release From Microglia

LPS endotoxin derived from gram-negative bacteria induces a large amount of TNF release via toll-like receptor 4 (TLR4) in microglia and macrophages. Such unregulated TNF release should cause inflammation and neuronal destruction. On the other hand, extracellular ATP stimulates the release of TNF from rat microglia via activating $P2X_7$ receptors (Hide et al., 2000), and this TNF release seems to be well regulated and to be neuroprotective (Suzuki et al., 2004). To investigate whether nicotine could modulate such microglial cell function, we examined the effects of nicotine on TNF release from microglia activated by LPS (1 ng/ml), ATP (1 mM), or the $P2X_7$ receptor agonist BzATP (100 μM). Nicotine significantly inhibited LPS-induced TNF release in a concentration-dependent manner (Fig. 1A), confirming a previous report (Shytle et al., 2004). Unlike LPS stimulation, however, nicotine significantly enhanced the release of TNF in ATP- or BzATP-stimulated microglia (Fig. 1B,C). These results indicate that nicotine might control microglial cell function toward neuroprotective by suppressing LPS-stimulated massive TNF release and enhancing ATP-induced protective TNF release.

Nicotine Modulates TNF Release Via Activation of α7 nAChRs

To clarify which subtype of nAChRs is responsible for modulation of TNF release in microglia, we examined the effects of methyllycaconitine (MLA), an α7 nAChR blocker, on nicotine-induced modulation of TNF release. MLA (10 nM) reversed these bidirectional actions of nicotine, namely, the inhibition of LPS-induced TNF release and the increase of ATP-stimulated TNF release (Fig. 2A,B). MLA did not affect LPS- or ATP-induced TNF release by itself. These results suggest that nicotine modulates TNF release at least through activation of α7 nAChRs. The expression of α7 nAChRs was recently shown in mouse microglia (Shytle et al., 2004). In this study, we also confirmed the expression of α7 nAChR protein by Western blotting and their mRNA expression by nested RT-PCR in primary rat brain microglia (Fig. 2C,D).

Microglial α7 nAChRs Do Not Function as Ligand-Gated Ion Channels but Induce Ca^{2+} Release From Intracellular Ca^{2+} Stores Through PLC and IP_3 Pathway

It is reported that neuronal α7 nAChRs are ligand-gated ion channels with high permeablity to Ca^{2+}, and the activation of these receptors by nicotine induces Ca^{2+} influx (Albuquerque et al., 1995). In rat microglia, nico-

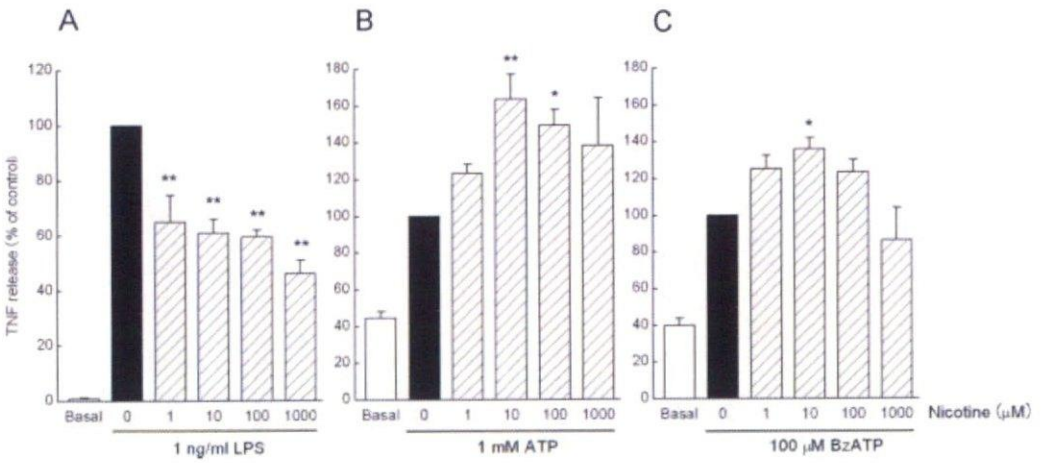

Fig. 1. Effects of nicotine on LPS-, ATP-, or BzATP-stimulated TNF release in microglia. The cells were treated with nicotine for 10 min and stimulated with 1 ng/ml LPS (**A**), 1 mM ATP (**B**), or 100 μM BzATP (**C**) for 3 hr. The released TNF was measured by ELISA. Values are expressed as mean ± SEM of percentage release compared with LPS or ATP/BzATP alone from three independent experiments. Values of 100% for the release of TNF in LPS-stimulated, ATP-stimulated, and BzATP-stimulated microglia were 11.7 ± 3.7 ng/10^6 cells, 0.42 ± 0.03 ng/10^6 cells, and 0.49 ± 0.09 ng/10^6 cells, respectively. $*P < 0.05$, $**P < 0.01$ vs. control (ANOVA with Dunnett's posttest).

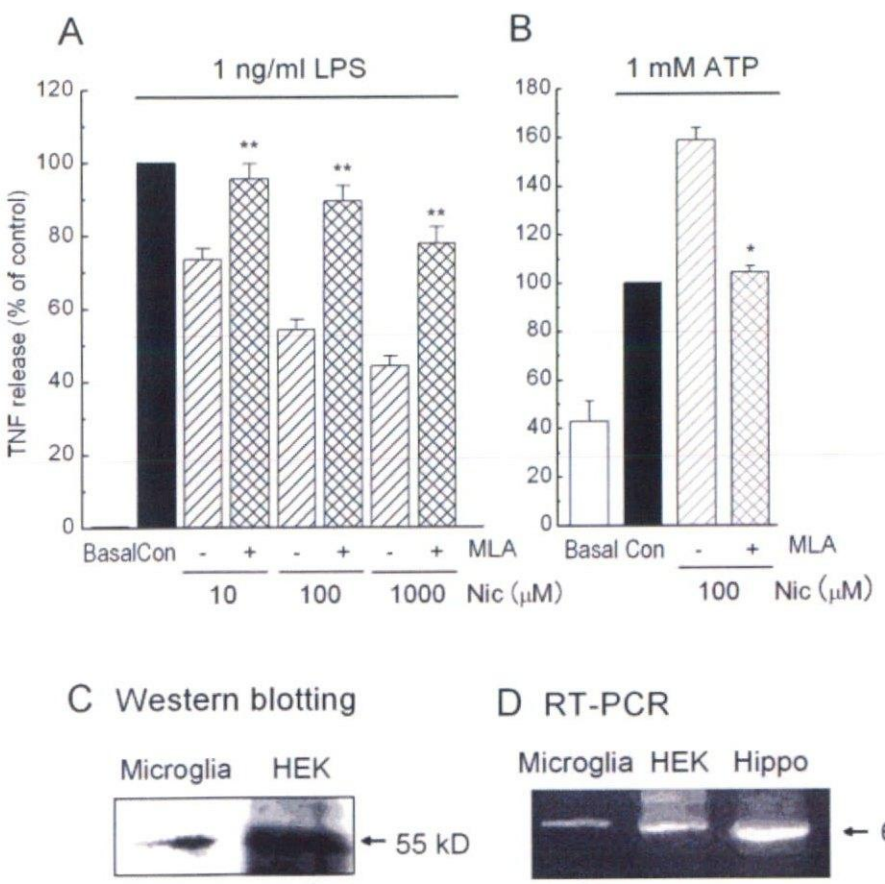

Fig. 2. The nicotine modulations of TNF release are mediated via α7 nAChRs expressed in microglia. **A,B:** Effects of methyllycaconitine (MLA), a specific antagonist of α7 nAChRs, on LPS- or ATP-induced TNF release from nicotine-treated microglia. The cells were treated with 10 nM MLA for 10 min before addition of nicotine, then stimulated with 1 ng/ml LPS (A) or 1 mM ATP (B) for 3 hr. The released TNF were measured by ELISA. Values are expressed as mean ± SEM of percentage of release compared with LPS alone from three independent experiments. Values of 100% for the release of TNF in LPS- and ATP-stimulated microglia were 20.5 ± 1.9 ng/10^6 cells (A) and 466.5 ± 15.6 pg/10^6 cells (B), respectively. $*P < 0.05$, $**P < 0.01$ compared with each nicotine-treated control (ANOVA with Dunnett's posttest). **C,D:** Protein and mRNA expression of α7 nAChRs in primary rat brain microglia. C: Western blotting. Cell lysates were analyzed with specific antibody against α7 nAChR. HEK 293 cells overexpressing α7 nAChRs were used as a positive control. D: Nested RT-PCR with primers specific for the α7 subunit as described in Materials and Methods.

tine induced a rapid and transient increase in the concentration of cytosolic Ca^{2+} (Fig. 3A). This Ca^{2+} response was strongly blocked by 10 nM MLA, an α7 nAChR blocker (Fig. 3B), showing that microglial α7 nAChRs are functional. Another selective α7 nAChR antagonist, α-bungarotoxin (10 nM), also blocked this response (Fig. 3C). Unexpectedly, however, the nicotine-elicited transient increase in intracellular Ca^{2+} concentration was not affected even in the absence of extracellular Ca^{2+} (Fig. 3D). Furthermore, nicotine-induced Ca^{2+} response

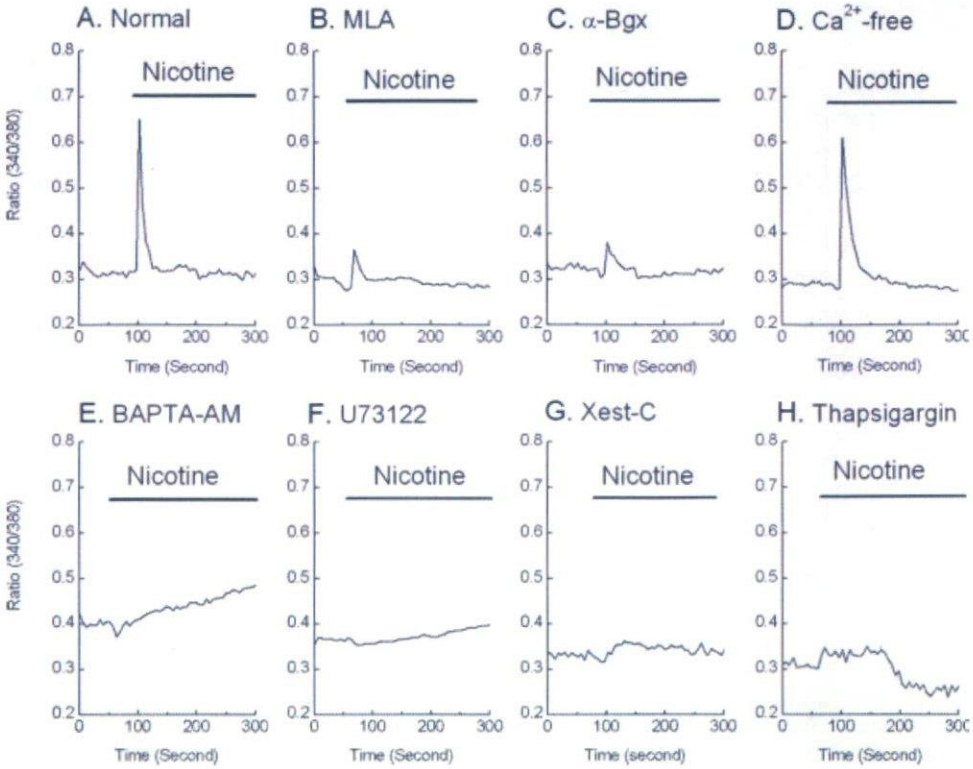

Fig. 3. Ca^{2+} response in nicotine-stimulated microglia. Fura-2-loaded cells were stimulated with 1 mM nicotine in Hank's buffer. The traces shown are representative of mean increase in $[Ca^{2+}]_i$ of 30 cells in each culture. The cells were stimulated with 1 mM nicotine (**A**) or stimulated with 1 mM nicotine in the presence of 10 nM MLA (**B**) or 10 nM α-bungarotoxin (**C**), selective inhibitors of α7 receptor, in the absence of extracellular Ca^{2+} (**D**), in the presence of 50 μM BAPTA-AM, an intracellular Ca^{2+} chelator (**E**); 5 μM U73122, an inhibitor of PLC (**F**); 100 nM xestospongin C, an inhibitor of IP_3 receptors (**G**); or 1 μM thapsigargin, an inhibitor of the endoplasmic reticulum Ca^{2+}-ATPase (**H**). Similar results were obtained in at least three independent experiments.

was markedly inhibited by 50 μM BAPTA-AM, an intracellular Ca^{2+} chelator, and 5 μM U73122, a selective inhibitor of PLC (Fig. 3E,F). In addition, nicotine-induced Ca^{2+} increase was also abolished by 100 nM xestospongin C, an IP_3 receptor antagonist, and by the store depletion with 1 μM thapsigargin, a Ca^{2+}-ATPase inhibitor (Fig. 3G,H). All these results suggest that, unlike neuronal α7 nAChRs as typical ion channels, microglial α7 nAChRs might link to the activation of PLC and the release of Ca^{2+} from IP_3-sensitive intracellular Ca^{2+} stores.

To explore further the properties of α7 nAChRs in microglia, we tried to detect nicotine-elicited currents by a whole-cell patch clamp technique. In our previous studies (Matsubayashi et al., 1997, 1998, 2004), this technique successfully detected nicotine-induced currents via α7 nAChRs in neurons from hippocampus and substantia nigra of rats. Interestingly, in microglia, no nicotine-induced currents were observed (Fig. 4A), although ATP-stimulated currents were detected in all the cells tested (Fig. 4B). These results suggest again that α7 nAChRs may function like metabotrophic receptors rather than ligand-gated ion channels in microglia.

Furthermore, to investigate whether such novel signaling generated through α7 nAChRs may be involved in the modulation of TNF release, we examined the effects of xestospongin C, a blocker of IP_3 receptors, on nicotine-induced suppression of LPS-stimulated TNF release. Xestospongin C (100 nM) completely abolished the suppression of LPS-induced TNF release by nicotine in microglia (Fig. 5). Therefore, the Ca^{2+} release from intracellular Ca^{2+} stores stimulated via α7 AChRs may plays

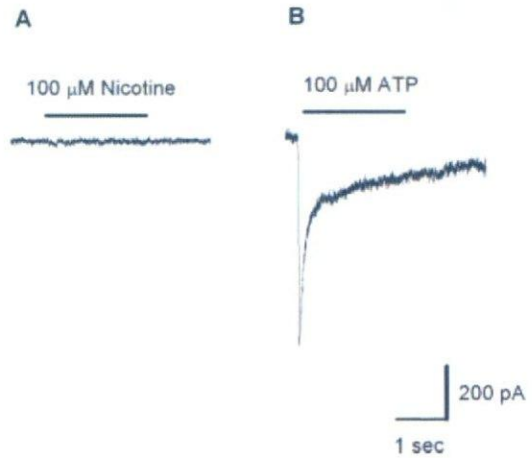

Fig. 4. Lack of nicotine-induced currents of rat microglia. **A:** Nicotine (100 μM) was delivered to microglia, and the whole-cell currents were recorded. **B:** ATP (100 μM) was applied to the same cells after nicotine stimulation. Similar results were obtained at least in 20 cells.

an important role in the modulation of LPS-induced TNF release.

Nicotine Selectively Inhibits LPS-Induced Activation of JNK and p38 MAPK, but Not ERK, and Modulates a Posttranscriptional Step of TNF Synthesis

To investigate the mechanism underlying the modulation of LPS-induced TNF release via α7 AChRs, we

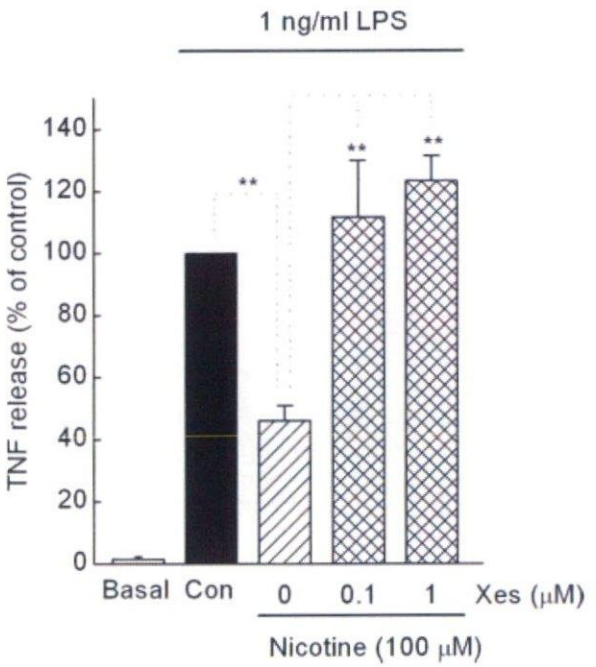

Fig. 5. Effects of xestospongin C, a blocker of IP_3 receptor, on nicotine-induced inhibition of TNF release in LPS-stimulated microglia. The microglia were treated with 0.1 μM or 1 μM xestospongin C for 30 min and treated with nicotine for another 10 min. Then, the cells were stimulated with 1 ng/ml LPS for 3 hr. The released TNF was measured by ELISA. Values are expressed as mean ± SEM of percentage of release compared with LPS alone from three independent experiments. Value of 100% for the release of TNF in LPS-stimulated microglia was 23.2 ± 4.0 ng/10^6 cells. $^{**}P < 0.01$ compared with the control or nicotine-treated control as indicated with dotted lines (ANOVA with Dunnett's posttest).

examined whether nicotine could regulate LPS-induced MAP kinase activation, because all three members of the MAPK family (ERK, JNK, and p38) are shown to be involved in LPS-induced TNF production (Bhat et al., 1998; Lee et al., 2000). We also confirmed that all inhibitors, 10 μM U0126 (which inhibits MEK), 30 μM SP600125 (which inhibits JNK), and 15 μM SB203580 (which inhibits p38) significantly suppressed the release of TNF (Fig. 6A). In the case of TNF mRNA expression, U0126 caused a marked reduction, whereas neither SP600125 nor SB203580 did so (Fig. 6B). These results suggest that, although three kinases play critical roles in TNF release, they appear to have different modes; ERK acts to regulate transcription of the TNF gene, and p38 and JNK act posttranscriptionally. Nicotine was capable of selectively inhibiting the LPS-induced activation of JNK and p38 but appeared to have little effect on the activation of ERK (Fig. 6D). Nicotine itself did not cause the activation of any MAP kinases (data not shown). In accordance with these results, nicotine did not change LPS-induced TNF mRNA expression levels (Fig. 6C). Therefore, nicotine may modulate the release of TNF through regulating the posttranscriptional steps implicating JNK and p38 in LPS-stimulated microglia.

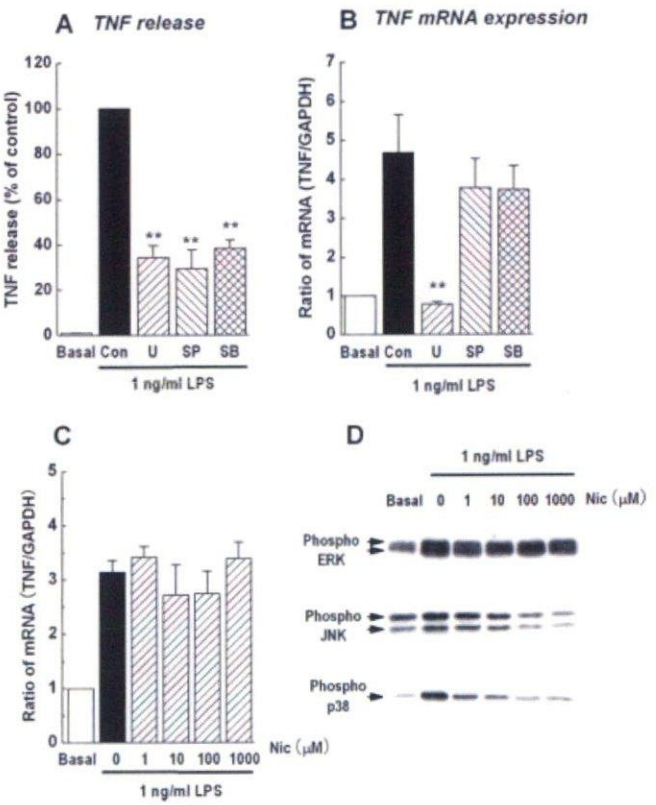

Fig. 6. Effects of U0126, SP600125, and SB203580 on LPS-induced TNF release and mRNA expression (**A,B**) and effects of nicotine on LPS-induced TNF mRNA expression (**C**) and on LPS-induced activation of ERK, JNK, and p38 MAP kinase (**D**) in microglia. A: The cells were treated with 10 μM U0126 (U), 30 μM SP600125 (SP), or 15 μM SB203580 (SB) for 15 min and stimulated with 1 ng/ml LPS for 3 hr. The released TNF were measured by ELISA. Values are expressed as mean ± SEM of percentage of release compared with LPS alone from three independent experiments. Values of 100% for the release of TNF in LPS-stimulated microglia were 12.5 ± 2.6 ng/10^6 cells. $^{**}P < 0.01$ vs. control (ANOVA with Dunnett's posttest). B: The cells were treated with 10 μM U0126 (U), 30 μM SP600125 (SP), or 15 μM SB203580 (SB) for 15 min and stimulated with 1 ng/ml LPS for 1 hr. The expression of TNF mRNA was quantified by real-time RT-PCR. Values are shown as the ratio of TNF mRNA vs. GAPDH mRNA. Data are expressed as mean ± SEM of ratio of expression compared with LPS alone from three independent experiments. $^{**}P < 0.01$ vs. control (ANOVA with Dunnett's posttest). C: The cells were treated with nicotine for 10 min and stimulated with 1 ng/ml LPS for 1 hr. The expression of TNF mRNA was quantified by real-time RT-PCR. Values are shown as the ratio of TNF mRNA vs. GAPDH mRNA. Data are expressed as mean ± SEM of ratio of expression compared with LPS alone from three independent experiments. D: The cells were treated with nicotine for 10 min and stimulated with 1 ng/ml LPS for 30 min. The phosphorylated (active) ERK, JNK, and p38 were detected by Western blotting with antibodies that recognize phosphorylated enzymes. The levels of each total MAP kinase were confirmed to be identical for each lane. Similar results were obtained in at least three independent experiments.

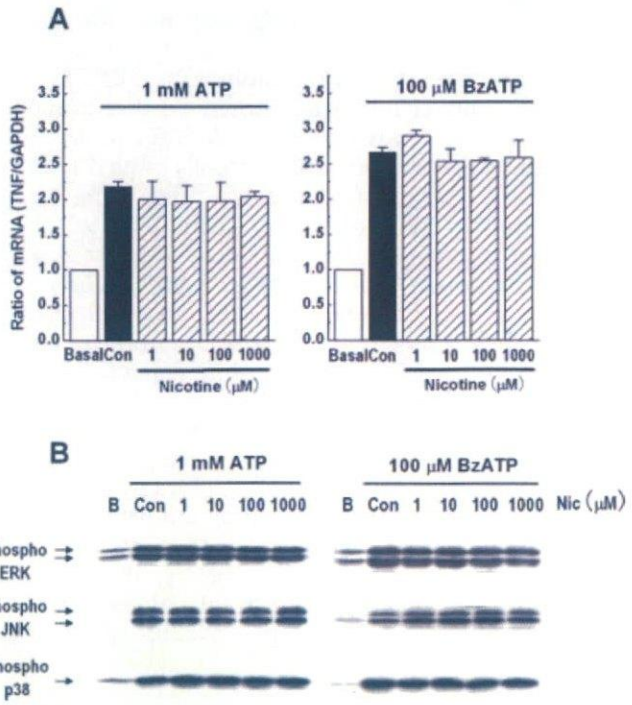

Fig. 7. Effects of nicotine on ATP- or BzATP-induced TNF mRNA expression and ATP- or BzATP-induced activation of ERK, JNK, and p38 MAP kinase in microglia. **A:** The cells were treated with nicotine for 10 min and stimulated with 1 mM ATP or 100 μM BzATP for 1 hr. The expression of TNF mRNA was quantified by real-time RT-PCR. Values are shown as the ratio of TNF mRNA vs. GAPDH mRNA. Data are expressed as mean ± SEM of ratio of expression compared with ATP or BzATP alone from three independent experiments. **B:** The cells were treated with nicotine for 10 min and stimulated with 1 mM ATP or 100 μM BzATP for 10 min. The phosphorylated (active) ERK, JNK, and p38 were detected by Western blotting with antibodies that recognize phosphorylated enzymes. The levels of each total MAP kinase were confirmed to be identical for each lane. Similar results were obtained in at least three independent experiments.

Nicotine Does Not Affect the Activation of Any MAP Kinases in ATP- or BzATP-Stimulated Microglia

We previously reported the critical roles of each MAPK in ATP-stimulated TNF production; both ERK and JNK are involved in the regulation of TNF mRNA expression, and p38 is involved in the nucleocytoplasmic transport of TNF mRNA (Suzuki et al., 2004). Unlike LPS stimulation, nicotine did not affect the activation of any MAP kinases in ATP- or BzATP-stimulated microglia (Fig. 7B). Furthermore, nicotine did not change the mRNA expression of TNF after 1 hr stimulation with 1 mM ATP or 100 μM BzATP (Fig. 7A). These results suggest that nicotine enhances $P2X_7$ receptor-mediated TNF release, possibly via a posttranscriptional event, but not MAPK modification.

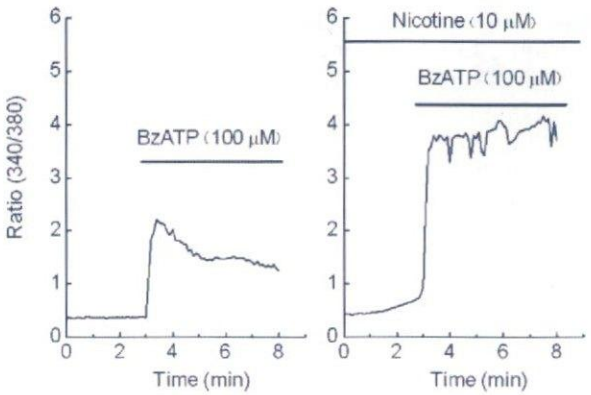

Fig. 8. Nicotine enhances BzATP-induced Ca^{2+} signal in microglia. Fura-2-loaded cells were treated with 10 μM nicotine for 10 min and stimulated with 100 μM BzATP. The traces shown are representative of mean increase in intracellular Ca^{2+} concentrations of 30 cells in each culture. Similar results were obtained in six independent experiments.

Nicotine Enhances $P2X_7$ Receptor-Mediated Ca^{2+} Influx in Microglia

To explore the mechanism underlying the enhancement of TNF release by nicotine in $P2X_7$ receptor-activated microglia, we examined the effect of nicotine on Ca^{2+} response mediated by $P2X_7$ receptor agonist BzATP (Fig. 8). The most effective concentration (10 μM) of nicotine for increasing ATP-induced TNF release (Fig. 1B,C) was used to treat the cells. This low concentration of nicotine no longer elicited detectable Ca^{2+} response by itself but after 10 minutes significantly enhanced Ca^{2+} increase in response to BzATP. Therefore, nicotine may increase TNF release by enhancing $P2X_7$ receptor-mediated Ca^{2+} influx.

DISCUSSION

In this study, we present the following experimental evidence regarding the action of nicotine on microglial cell function. First, in rat brain primary cultured microglia, nicotine modulates the release of TNF, a multifunctional cytokine via α7 nAChRs, in a different manner depending on the nature of the stimulants; namely, negatively for LPS stimulation and positively for ATP or BzATP stimulation. Second, microglial α7 nAChR may not function as ligand-gated ion channels but instead couple to the activation of PLC and Ca^{2+} release from IP_3-sensitive intracellular Ca^{2+} stores. This novel signaling is likely involved in nicotine modulation of LPS stimulation. Third, nicotine-induced suppression of TNF release seems to occur at a posttranscriptional step by interfering with the activation of JNK and p38. Finally, nicotine enhanced protective TNF release through enhancing $P2X_7$ receptor function, without affecting MAP kinase activation.

Upon ischemia and trauma, microglia secrete excessive amounts of TNF and induce inflammatory destruction in the brain (Barone et al., 1997). Most neurodegenerative diseases, such as Alzheimer's disease and Parkinson's disease, are also associated with neuronal inflammation and